

Coherent QCD phenomena in the Coherent Pion-Nucleon and Pion-Nucleus Production of Two Jets at High Relative Momenta

L. Frankfurt

*School of Physics and Astronomy,
Tel Aviv University, 69978 Tel Aviv, Israel*

G. A. Miller

*Department of Physics, Box 351560
University of Washington
Seattle, WA 98195-1560, U.S.A.*

M. Strikman

*Department of Physics, Pennsylvania State University,
University Park, PA 16802, USA*

We use QCD to compute the cross section for high-energy coherent production of a dijet (treated as a $q\bar{q}$ moving at high relative transverse momentum, κ_t) from a nucleon and a nuclear target. The direct evaluation of the relevant Feynman diagrams shows that, in the target rest frame, the space-time evolution of this reaction is dominated by the process in which the high κ_t $q\bar{q}$ component (point like configuration) of the pion wave function is formed before reaching the target. This point like configuration then interacts through two gluon exchange with the target. In the approximation of keeping the leading order in powers of α_s and in the leading log approximation in $\alpha_s \ln(\kappa_t^2/\Lambda_{QCD}^2)$, the amplitudes for other processes are shown to be smaller by at least a power of α_s and/or powers of Sudakov-type form factors and the small probability, w_2 , to find a $q\bar{q}$ pair with no gluons at an average separation between constituents. Thus the high κ_t component of pion wave function, including the contribution of Gegenbauer polynomials of rank $n > 0$, can be measured in principle at sufficiently large values of κ_t^2 . At large values of κ_t^2 , the resulting dominant amplitude is proportional to $z(1-z)\alpha_s(k_t^2)\kappa_t^{-4}(\ln \frac{\kappa_t^2}{\Lambda^2})^{\frac{CF}{\beta}}$ (z is the fraction light-cone (+) momentum carried by the quark in the final state, β is the coefficient in the running coupling constant) times the skewed gluon distribution of the target. For pion scattering by a nuclear target, this means that at fixed $x_N = 2\kappa_t^2/s$ (but $\kappa_t^2 \rightarrow \infty$) the nuclear process in which there is only a single interaction is the most important one to contribute to the reaction. Thus in this limit color transparency phenomena should occur—initial and final state interaction effects are absent for sufficiently large values of κ_t . These findings are in accord with the recent experiment performed at FNAL. We also re-examine a potentially important nuclear multiple scattering correction which is positive and varies as the length of the nucleus divided by an extra factor of $1/\kappa_t^4$. The meaning of the signal obtained from the experimental measurement of pion diffraction into two jets is also critically examined and significant corrections are identified. We show also that for values of κ_t achieved at fixed target energies, dijet production by the electromagnetic field of the nucleus leads to an insignificant correction which gets more important as κ_t increases. We explain also that the same regularities are valid for photo-production of forward light quark dijets.

I. INTRODUCTION

The theory of strong interactions, QCD, contains many specific predictions regarding the space-time evolution of high energy coherent processes. A review describing the many interesting qualitative results that have been obtained in this rapidly developing field is provided in Ref. [1]. The aim of this paper is to use a specific example of a completely calculable process to demonstrate the general properties of space-time evolution of hard exclusive processes in QCD. In particular, we consider a process in which a high momentum (~ 500 GeV) pion undergoes a coherent interaction with a nucleus in such a way that the final state consists of two jets (JJ) (formed by a $q\bar{q}$ pair) moving at high transverse relative momentum greater than about 2 or 3 GeV. The process of two-jet production was first discussed for both photon and pion projectiles interacting with a nucleon target [2], and Ref. [3] introduced the possibility of using this process to probe the nuclear filtering of small color dipoles. Estimates of Ref. [3] found that for heavy nuclei, nuclear filtering causes the exclusive dijet production to decrease exponentially as κ_t^2 increases. Hence an overall increase of the total diffractive cross sections was suggested as a good signature of the nuclear filtering of small

size configurations [4]. In [5] we presented the first application of QCD to the process of dijet production at large κ_t by generalizing QCD factorization theorems, predicted a nuclear dependence which is qualitatively different from that suggested in [3], and a κ_t dependence which differs by a power of κ_t^2 from [2] and qualitatively from that discussed in [3]. We also argued that this process can be used to directly measure the behavior of the $q\bar{q}$ component of the pion's light cone wave function for large values of κ_t .

If one wishes to describe hard diffractive processes, it is important to realize that the effective number of bare particles in the light cone wave function of the projectile depends strongly on the longitudinal distances involved. If these distances are small, and the process involves high momentum transfer, (as occurs in computing hadron electromagnetic form factors) the main contribution originates from the Fock component of the hadron wave function containing the minimal number of constituents. On the contrary, if the longitudinal distances are sufficiently large, the minimal Fock component (a $q\bar{q}$ pair in our case) will develop additional components such as $q\bar{q}$ pairs and gluons. Thus for those processes in which infinite longitudinal distances are involved, the number of partons in the light cone wave function of the projectile would always be infinite. For processes initiated by a spatially small colorless dipole, using the QCD factorization theorem allows one to trace the origin of wee partons (carrying a small fraction of the momenta) as arising from the space-time evolution of the projectile's minimal Fock component, and to include these effects in the (skewed) parton distribution of the target.

We now discuss the basic physics of the dijet production process. The selection of the final state to be a $q\bar{q}$ pair plus the nuclear ground state causes the $q\bar{q}$ component of the pion wave function to dominate the reaction process. At very high beam momenta, the pion breaks up into a $q\bar{q}$ pair with large κ_t well before hitting the nucleus. The dominance of this starting point is verified in the present work. Note also the crucial feature that for values of x which are not very small, so that the leading twist approximation is valid for the small dipole - target interaction, a spatially small wave packet of quarks and gluons remains small as it moves through the target. This leads to a dominance of the effects of large transverse momenta, and allows the factorization of the hard physics from the soft physics. On the other hand, for very small values of x , the packet lives so long that it would expand to a normal hadronic size causing the initial state interaction to become similar to the soft one. Moreover, a rapid increase of PQCD amplitudes with energy leads to the violation of QCD evolution equation at rather small values of x , and to the disappearance of the characteristic physics of the interaction of a small dipole. Thus QCD predicts different calculable dependencies of the cross section of the diffractive dijet production on atomic number, on κ_t and z in different regions of the $\ln \kappa_t^2/\Lambda_{QCD}^2$, $\ln 1/x$ plane.

Thus two large parameters s and κ_t^2 are present, and this feature will enable us to demonstrate the dominance of Feynman diagrams of a very few specific topologies, and to evaluate them. The result of calculations can be represented in the form of a generalized QCD factorization theorem, valid for the set of Feynman diagrams corresponding to the leading power of s and the minimal power of $1/\kappa_t^2$ and α_s at fixed values of $\alpha_s \ln \kappa_t^2/\Lambda_{QCD}^2$. Our calculation relies heavily on the well-known theoretical observation that amplitudes of many high energy processes (such as that in the parton model, multi-peripheral processes and those involving the Pomeron) are dominated by ladder diagrams [6,7]. This property has been proved using the approximation of including the terms of lowest order α_s and all powers in $\alpha_s \ln Q^2/\Lambda_{QCD}^2$ [8,9] and/or $\alpha_s \ln 1/x$ [6,10]. The dominance of ladder diagrams makes it possible to absorb the effects of the leading terms in $\ln \kappa_t^2/\Lambda_{QCD}^2$ and $\ln 1/x$ into the dipole-target interaction, and/or into the target's skewed parton distributions. Furthermore, one may classify and analyze those diagrams of leading power of α_s which are relevant for the pion transition into two jets. This leads to a selection rule: the t -channel exchanges with vacuum quantum numbers (positive charge parity) should dominate. Thus we will calculate an amplitude which is symmetric under the transposition $s \leftrightarrow u$. Negative charge parity contributions (such as effects of the odderon) are neglected. There is another group of correction terms of the form $\alpha_s \ln \kappa_t^2/\Lambda_{QCD}^2$ which arises from radiative effects in the pion wave function. The ladder structure of the dominant diagrams makes it possible to include these terms into QCD evolution of pion wave function and structure functions of the target will not change the structure of formulas deduced by considering skeleton diagrams calculated within the approximation of keeping leading powers of α_s ; their only influence is to introduce the effects of evolution in κ_t^2 into the relevant parton distributions and into high k_t behavior of the pion wave function. Indeed, our theoretical analysis heavily relies upon specific properties of skewed parton distributions and of minimal Fock component of pion wave function. Note also that, for small values of x , and large values of Q^2 , the skewed parton distribution of a target nucleon or nucleus is calculable in QCD using the appropriate evolution equation and initial diagonal parton densities [11]. To simplify the calculations and especially the separation of the scales, we use an axial light-cone gauge, which reduces to the $A_- = 0$ gauge, in the target rest frame. This gives a high κ_t behaviour of fermion propagator and hard gluon exchange amplitude which have no infrared singularities. In this gauge, unphysical degrees of freedom are removed from the light cone pion wave function at least within the leading log approximation. Consequently, the separation of momentum scales can be easily made. On the contrary, in the gauge used in [46] the separation of scales and therefore derivation of the QCD evolution equation, although correct, is complicated by the need to account for the cancellation of the infrared divergences.

We want to stress that in the calculation of amplitudes of hard diffractive processes in the gauge where fermion propagators are infrared divergent one, should first remove infrared divergences and only then consider partons in the non-perturbative wave function to be on-mass-shell.

These technical considerations lead to some simple results for situations, such as ours, in which the momentum transfer to the target nucleus is very small (almost zero for forward scattering). In this case, the dominant source of high momentum must be the gluonic interactions between the pion's quark and anti-quark. This is also justified in the present work. Because κ_t is large, the quark and anti-quark must be at small separations—the virtual state of the pion is a point-like-configuration [12]. But the coherent interactions of a color neutral point-like configuration are suppressed (at fixed x_N , $\kappa_t^2 \rightarrow \infty$), for the processes which involve small transfers of momentum to the target, by the cancellation of gluonic emission from the quark and anti-quark [13,3,12] and /or from the $q\bar{q}g$ state.—see the discussion in the section II.D.

Furthermore, the strength of the interaction with the target is proportional to the square of the transverse separation distance between the quark and anti-quark. Thus the interaction with the nucleus is very rare, and the pion is most likely to interact with only one nucleon. The result is that in this process the initial π and the final $q\bar{q}$ pair do not get absorbed by the target, as would typically occur in a low momentum transfer process. Thus initial and final state interactions are suppressed and color transparency unambiguously follows. As the values of x are decreased, the qualitative physics changes gradually. The increase of the effective size of the small color-dipole leads to the increase of the influence of initial state interactions, and to a contribution of nuclear shadowing which enters at leading twist. For even smaller values of x , the leading twist approximation breaks down.

Our treatment of the reaction process in terms of a separate wave function and interaction pieces provides a new example of how the QCD factorization theorem works for high energy processes involving two large variables: s, κ_t [12]. For this coherent process, the forward scattering amplitude is almost proportional to the number of nucleons, A , and the cross section varies as A^2 . The forward angular distribution is difficult to observe, so one integrates the angular distribution, and the A^2 variation becomes $\approx \frac{A^2}{R_A^2/3+B_N} \propto \frac{A^{4/3}}{1+0.45A^{-2/3}} \approx A^{1.37}$. Here $B_N \approx 4.5\text{GeV}^{-2}$ is the slope of the t dependence of the cross section of a hard diffractive process as determined by data for electroproduction of vector mesons. This very rapid variation represents a prediction of a very strong enhancement which occurs via the suppression of those interaction processes which usually reduce the cross section. Our interest in this curious process has been renewed recently by exciting experimental progress [14].

Three key predictions of our paper [5] are confirmed by the E791 data:

- The result from the E-791 experiment comparing Pt and C targets that the coherent cross section for small momentum transfer to the nucleus varies as $\sim A^{1.55 \pm 0.05}$, is close to our predictions, see Section V. This variation is much stronger than seen in soft diffraction of pions by nuclei $\sim A^{0.8}$ [12,15], which is qualitatively different from the behavior $\sim A^{1/3}$ suggested in Ref. [3]. This A-dependence is somewhat more rapid than that predicted by color transparency theory for $A \rightarrow \infty$. For moderately large values of A , small effects discussed in Sect. V tend to increase the A dependence. This may be understood as a result of the experimental trigger not excluding a small but calculable admixture of the effects of nuclear disintegration processes which lead to similar dependence of cross section on t . Furthermore, it is an unusual feature [5] of the present process that final state interactions of the point-like configuration tend to increase the A -dependence. Sect. V also contains a discussion of the changes of the A-dependence due to the effects of nuclear shadowing on the gluon density.
- The dependence of the cross section $\propto z^2(1-z)^2$ on the fraction of momentum z carried by one of the jets is consistent with our prediction.
- The cross section $d\sigma/d\kappa^2$ falls as κ_t^{-n} with $n = 10.2 \pm 0.4$ (stat) ± 0.3 (sys), for $\kappa_t \geq 1.25\text{GeV}$ and as $n = 7.5 \pm 2.0$ for $\kappa_t \geq 1.8\text{ GeV}$. This should be compared to the prediction of $n = 8$ [5]. For smaller values of κ_t soft QCD phenomena, such as production of $q\bar{q}g$ jets, should be important. See the discussion in Sect. III A.

The purpose of the present work is to rederive and confirm our earlier theoretical results with a more extensive analysis. The derivation of our leading term [5] directly from QCD by generalizing a QCD factorization theorem of Ref. [16] was presented in Ref. [17], and this is explained more fully now. But here we go further by verifying the assumption that the point-like-configuration is indeed formed well before the projectile reaches the nucleus. In the derivation we shall explain that several different amplitudes, which seem to be of the same or lower order in α_s as the leading one described above really are very small after proper account of the suppression of radiation collinear to pion momentum direction.

We also update our study of the leading multiple-scattering correction, which is positive because the strength of the final state interaction decreases with decreasing size of the dipole [5], and we study the most important competing electromagnetic process. Some specific features of the experimental extraction of the coherent part of the cross section are also explained. Still another feature involves the soft interaction between the dipole and the target. This was

at first derived to be proportional to the gluon density of the nucleus [18]. However, there is a non-zero momentum transfer to the nucleus, so it is actually the skewed gluon density that enters. The skewedness of gluon distribution in the nuclear target leads to a small, calculable correction to the predicted A dependence [19] and absolute value [11] which changes the detailed nature of our results but not the qualitative features.

Our main results are summarized by the following formula, valid in the leading log approximation, for the differential cross section of diffractive dijet production by nuclei:

$$\frac{d\sigma(\pi + A \rightarrow 2jet + A)(q_t = 0)}{dtdz d^2\kappa_t} = \frac{(1 + \eta^2)}{4\pi(2\pi)^3} \left(\int d^2r_t \frac{d\beta}{\beta} \exp i(\mathbf{\kappa}_t \cdot \mathbf{r}_t) \cdot \right. \\ \left. (\alpha_s \pi^2 / 3) \int d^2k_{1t} [2\chi_\pi(z, r_t) - \exp(-i(\mathbf{r}_t \cdot \mathbf{k}_{1t})\chi_\pi(z - \beta, r_t) - \exp(i(\mathbf{r}_t \cdot \mathbf{k}_{1t})\chi_\pi(z + \beta, r_t))] \frac{f_A(x_1, x_2, \beta s, k_{1t}^2)}{k_1^2 k_2^2} \right)^2, \quad (1)$$

where by definition \mathbf{r}_t is the transverse distance between the pion's quark and anti-quark, $\frac{\chi_\pi(z, k_t)}{d_f(k_t)} \equiv \int d^2r_t \exp i(\mathbf{k}_t \cdot \mathbf{r}_t)\chi_{1,\pi}(z, r_t)$ and $x_1 G_A(x_1, x_2, Q^2) = \int_0^{Q^2} d^2l \int_{\beta_0}^1 \frac{d\beta}{\beta} d^2l \frac{f_A(x_1, x_2, \beta s, l^2) k_{1t}^2}{k_1^2 k_2^2}$ (f_A can be denoted as the un-integrated skewed nuclear gluon density), k_i are four momenta of two exchanged gluons, (see Fig. 1), and $k_{1t} = \kappa_t - l_t$.

Here $d_f(\kappa_t^2)$ is the renormalization factor for the quark Green function $S_f(k)$ in the hard regime where

$$S_f(k) = \frac{d_f(\kappa^2)}{\hat{k}}, \quad (2)$$

for $k^2 = \kappa^2$. The quantity β_0 is a complicated function involving the transverse momenta of the quarks within the pion, and in the region giving the dominant contribution $\beta_0 \propto \kappa_t^2/s$. The quantity η is the ratio of the real to imaginary part of the $q\bar{q}$ -target scattering amplitude. In Eq. (1), $\chi(z, r_t)$ includes both the non-perturbative $q\bar{q}$ component and its high momentum tail. This function therefore involves distances significantly smaller than average hadronic inter-quark distances. The actual distances involved in the largest contributions is one of subjects investigated here.

Equation (1) is derived in two steps. First we demonstrate the dominance of the Feynman diagrams of Fig. 1 and then evaluate these diagrams. The factorization of the hard perturbative QCD part, related to the pion wave function, and $q\bar{q}$ pair arising from softer QCD, described by skewed parton distributions (the dominance of the diagrams of Fig. 1) is another form of the QCD factorization theorem derived in [16] for diffractive vector meson production in deep inelastic scattering DIS. The end point contribution - the Feynman mechanism ($-z \propto \frac{\Lambda_{QCD}^2}{\kappa_t^2}$) is suppressed as compared to the leading term by a set of factors: one power of $\frac{1}{\kappa_t^2}$, the square of the Sudakov-type form factor, by a form factor w_2 (which accounts for the very small probability to find a pion with q and \bar{q} at *average* distances without a gluon field) and by the overlap integral with final state. A detailed analysis of the end point contribution will be subject of a separate publication. It follows from QCD factorization theorems that the amplitude of hard processes can be represented as the convolution of the non-perturbative pion wave function and hard amplitude T . The virtualities of all particles in the s, u cuts of the amplitude T are large. Virtualities of those seemingly on-mass-shell particles are $\gg \Lambda_{QCD}^2$ but $\ll \kappa_t^2$. This is the condition which dictates the dominance of perturbative tail in the pion wave function at $\kappa_t^2 \rightarrow \infty$ but fixed $x = \kappa_t^2/\nu$. The amplitudes having different topology are radiative corrections involving extra powers of α_s . To elucidate the underlining physics we shall prove the dominance of the amplitude T_1 (see Fig. 1) by analyzing different contributions of many diagrams. A more general proof will be given elsewhere. In the leading $\ln \frac{Q^2}{\Lambda_{QCD}^2}$ and $\ln \frac{1}{x}$ approximations the dipole description can be used to simplify the above equation to the form:

$$\frac{d\sigma(\pi + A \rightarrow 2jet + A)(q_t = 0)}{dtdz d^2\kappa_t} = \frac{(1 + \eta^2)}{16\pi(2\pi)^3} \left[\Delta \left(\frac{\chi_\pi(z, \kappa_t)}{d_f(\kappa_t^2)} \right) \frac{\alpha_s \pi^2}{3} x_1 G_A(x_1, x_2, Q^2) \right]^2. \quad (3)$$

where $\chi_\pi(z, \kappa_t) \equiv 4\pi C_F \frac{\alpha_s(\kappa_t^2)}{\kappa_t^2} \sqrt{3} f_\pi z(1-z)$, Δ is the Laplacian in κ_t space, z is the fraction light-cone (+) momentum carried by the quark in the final state, $x_1 G_A(x_1, x_2, \kappa_t^2)$ is the skewed gluon density of the nucleus, x_1, x_2 are the fractions of target momentum carried by exchanged gluons 1 and 2, $x_1 - x_2 = M_{2jet}^2/s$, $x_2 \leq x_1$, and $\eta = ReF/ImF$ (with F as the dipole-nucleon scattering amplitude). Note that the resulting κ_t^{-8} dependence is a consequence of a kind of dimensional counting, as explained in Sect. II.

It is necessary to discuss the kinematic and dynamic limitations of our analysis. We require high beam energies so that the point-like configuration remains small as it passes through the nucleus, and we also require that κ_t be large enough so that the $q\bar{q}$ pair actually be in a point-like configuration. This situation corresponds to κ_t^2/s being held fixed for large values of κ_t^2 . For the experiment of Ref. [14] $\kappa_t \approx 2$ GeV, and $s = 1000$ GeV², so $x_N \equiv \frac{2\kappa_t^2}{s} \approx .008$.

There is another kinematic limit in which κ_t^2 is fixed and s goes to ∞ . At sufficiently small values of x_N , less than about $\frac{1}{2m_N R_A}$, the situation is very different because the $q\bar{q}$ dipole system is scattered by the collective gluon field of the nucleus. Nuclear modifications (enhancement) of the nuclear gluon density actually occurs at larger values of x_N corresponding to $x_N \sim 1/(2m_N r_{NN}) \sim 0.1$ (where $r_{NN} \sim 2$ fm is the mean inter-nucleon distance in nuclei [20–22]). But for values such that $x_N \leq \frac{1}{2m_N R_A}$ the nuclear gluon field is expected to be shadowed, leading to a gradual disappearance of color transparency (at a fixed scale (κ_t^2)). This is the onset of perturbative color opacity [5,23,24]. At even smaller values of x_N a new phenomenon has been predicted – the violation of the QCD factorization theorem [25]. Our present analysis is not concerned with this region of extremely small x_N . Another interesting phenomenon is the possibility of probing the decomposition of quark distribution amplitude in terms of Gegenbauer polynomials at sufficiently large values of κ_t^2 .

Some general features of our analysis appear in several different Sections, so it is worthwhile to discuss these here. The calculations of several amplitudes are simplified by the use of a general theorem. In the leading order in $1/\kappa_t^2$, the interaction of the $q\bar{q}$ occurs via the exchange of a two-gluon ladder with the target. It is important to note that the interaction of the $q\bar{q}$ pair with the target via the exchange of a larger number of gluons is suppressed by powers of $1/\kappa_t^2$. The proof of this statement follows [16] and heavily uses Ward identities. (To visualize the similarity with the situation considered in Ref. [16], it is instructive to neglect the effects of the odderon contribution, which is in any case small. Accounting for symmetry of amplitude on the transposition: $s \leftrightarrow u$ gives the possibility to consider the amplitude for the process $q\bar{q} + T \rightarrow \pi + T$, and to repeat the reasoning of [16] by parametrizing the momenta of exchanged gluons along dijet total momentum.) The QCD factorization theorem [16] predicts also that the interaction with the target via t -channel exchange by $q\bar{q}$ pair (which is expressed in terms of the skewed quark distribution) is not small at $x \geq 0.1$ and moderate κ_t where gluon distribution is not large [16,26]. At smaller $x \leq 10^{-2}$ and $\kappa_t^2 \geq 1.5 \text{ GeV}^2$ where the gluon distribution is large, as a result of x and Q^2 evolution, this term is a small correction to the exchange of the two-gluon ladder, see Eq. (60). So in this paper, we shall neglect this term. The two gluons are vector particles (bosons) in a color singlet state, so the dominant two-gluon exchange amplitude occurs in a channel which has positive charge and spatial parity, and is therefore even under crossing symmetry. Given this even amplitude, and the condition that we consider high energies $\nu \equiv 2p_\pi m_N$ and fixed small values of the momentum transfer t to the target, we may use the dispersion relation over invariant energy s at fixed t and fixed momenta of two jets to reconstruct full amplitude via the amplitude cut over intermediate states in s and u channels. In difference from the amplitudes of hard diffractive meson production, the amplitude for dijet production may have an imaginary part which varies with M_{2jet}^2 also. At the same time, within the approximations made here, the cut amplitude coincides with the imaginary part of the full amplitude. Furthermore, the relation discussed below makes it possible to reconstruct the real part of the amplitude from the imaginary part. For an amplitude corresponding to a slowly growing total cross section ($A \propto s^\alpha$, $\alpha \sim 1$) the relation is [27]

$$\frac{\text{Re}A(\nu, t)}{\text{Im}A(\nu, t)} = \frac{\pi}{2} \frac{\partial}{\partial \ln \nu} \ln \frac{\text{Im}A(\nu, t)}{\nu}. \quad (4)$$

This means that we may simply calculate the imaginary parts of any contribution to the scattering amplitude, as a function of s and u , with the full amplitude obtainable from Eq.(4). Furthermore, the imaginary part of the scattering amplitude, $\text{Im}A$ varies rather slowly with ν , leading to a small value of $\text{Re}A/\text{Im}A$. Thus $\text{Im}A$ dominates in the sum of diagrams. The possibility of considering only the imaginary part of the scattering amplitude simplifies the calculations enormously. The relevant intermediate states are almost on the energy-shell (virtuality of quark, anti-quark, gluon $\ll \kappa_t^2$) and one can use conservation of four-momentum to relate the momentum of the relevant intermediate states to that of the initial state.

There is another enormous simplification which is related to the issue of gauge invariance. The pion wave function is not gauge invariant, but the s, u cut parts of the amplitude $\pi + g \rightarrow JJ + g$, for two gluons in a color singlet state, are calculable in terms of amplitudes of sub-processes where only one gluon is off mass shell. For such amplitudes the Ward identities [28]– the conservation of color current– have the same form as the conservation of electromagnetic current in QED. In QED the current conservation identity has long been used to simplify calculations of high energy reactions [6]. We will often use the Ward identities [28] to extend the QED method to treat various contributions to our process. To be able to separate soft and hard scales one need to account for the cancellation of infrared divergences introduced by using the light-cone gauge $A_+ = 0$ [46]. Instead of accounting for this cancellation as in [46] we choose different gauges for the description of parton distributions in a nucleon, and for the amplitude pion fragmentation. This is legitimate within the region of applicability of leading log approximations. Within the chosen gauge, the hard gluon exchange amplitude and fermion propagator have no infrared divergence. Note also that after demonstrating the factorization of the hard QCD amplitude from the soft QCD amplitude, we may and will approximate the soft part of the pion wave function by a system of free $q\bar{q}$ [17]. However, we stress that this approximation is dangerous for evaluating the pieces of amplitudes dominated by soft physics especially if propagators contain infrared divergences.

In that case, this approximation violates Ward identities and the energy-momentum conservation law.

Additional common features arise from considering the relevant kinematics. In all of the two-gluon exchange diagrams we consider, Figs. 1-12, the target nucleon of momentum p emits a gluon of momentum k_1 and absorbs one of momentum k_2 . Conservation of four-momentum gives

$$k_1 - k_2 = p - p' = p_f - p_\pi, \quad (5)$$

in which p' and p_f are the final momenta of the target and the dijet. Taking the dot product of the above with p_π , for the large pion beam momentum relevant here, leads to the relation:

$$x_1 - x_2 = \frac{m_f^2 - m_\pi^2}{2p_\pi \cdot p} = \frac{m_f^2 - m_\pi^2}{\nu}, \quad (6)$$

where

$$x_{1,2} \equiv \frac{k_{1,2}^+}{p^+}, \quad (7)$$

and where m_f is the mass of the final 2jet system: $m_f = M_{2jet}$. Within the parton model approximation

$$x_2 > 0, \quad (8)$$

except the region of very small x_2 denoted the wee parton region. In the parton model this condition follows from the requirement that a parton knocked out of a nucleon should be kinematically separated from the rest of the target. Otherwise the amplitude should be suppressed by a power of κ_t^2 [7]. This suppression disappears at sufficiently high energies for which the parton wave function of a target develops wee partons.

Another important consequence of the positivity of “mass”² of partons in intermediate states Eq. (8) is that the fraction β of the pion’s (+) momentum carried by exchanged gluons should satisfy the condition:

$$1 > \beta > 0, \quad (9)$$

for our kinematics. The restriction $\beta \propto \kappa_t^2/\nu$ can be justified within the leading $\ln 1/x$ approximation only.

The results (6,8,9) are significant because they will be used in the evaluation of other diagrams. In particular the condition (8) is not fulfilled for the diagrams in which the transverse momenta of quarks within the pion wave function are significantly smaller than the observed transverse momenta of jets. This means that the quarks in the pion must have very high transverse momentum to satisfy Eq. (8). In this case, the quarks are closely separated and we may consider the configuration to be a point-like configuration. Such a restriction is operative in the kinematics for which the target wave function has no wee partons, i.e. for sufficiently large x_N . On the contrary, for sufficiently small values of x_N , the sign of x_2 becomes unimportant because the amplitude does not depend on the sign of wee parton momentum.

It is also worth emphasizing that the dominance of small size configurations in the projectile pion, so important to our analysis, is closely related to the renormalizable nature of QCD. This renormalizability implies, as extensively discussed below, that the selection of large transverse momentum final-state jets leads to a selection of the large transverse momenta of the quarks in the pion wave function, and also to some increase of transverse momenta of the exchanged gluons.

One also needs to realize that the emissions in the in-state and absorptions in the out-state combine in calculating the usual parton density to produce the renormalized parton density. Thus it is necessary to guarantee suppression of gluon radiation collinear to the pion direction in the initial, intermediate, and final states. Otherwise an exclusive process will be additionally suppressed by powers of the Sudakov type form factor. This is a stringent condition which suppresses the contribution of all other diagrams except that of Fig. 1 because for small values of x_N , the time and longitudinal distance intervals ($\sim 1/(2m_N x_N)$) are easily long enough to accommodate the radiation of a gluon. If a pion is in a spatially small quark-gluon component, collinear radiation is suppressed because color is highly localized in the plane transverse to the pion momentum. As a result (similar to the case of meson production by longitudinally polarized photons) there is no Sudakov form factor type suppression for such processes [29]. Note also that according to the QCD factorization theorem a pion in a small size configuration consists of $q\bar{q}$ pair accompanied by a coherent, relatively soft gluon field which follows the valence quarks without violation of coherence. This gluon field is included in the skewed gluon distribution.

Consider now the impact of the above-mentioned condition for the interactions of a pion in a large size $q\bar{q}$ configuration. The q , \bar{q} and gluons which start off far apart must end up with a $q\bar{q}$ pair close together in a final state

without collinearly moving gluons. In this case, the q and \bar{q} must undergo a high momentum transfer without emitting gluons collinear to the pion direction. But such processes are well known to be exponentially suppressed by double logarithmic Sudakov-type form factors. Only in the case of a compact $q\bar{q}$ pair, of a transverse size commensurate with the virtuality of a gluon bremsstrahlung, would the gluon radiation be small. A related suppression, evaluated in Sect. III is the very small probability w_2 of finding a pion with q and \bar{q} at *average* distances without a gluon field, if the probe has a resolution $\kappa_t^2 \gg \Lambda_{QCD}^2$. Note that under these conditions, in the typical parton configuration, gluons are experimentally observed to carry about $\sim 1/2$ of the pion momentum. Another example is pion scattering by a high momentum gluon field of a target. In the intermediate state there should be a strong collinear radiation along the pion direction because the color charge strongly changes its direction of motion, and there is no color charge nearby to compensate for this emission. This is similar to the effect of filling a gap in the case of color unconnected hard processes like Higgs production via $gg \rightarrow H$ in hadron-hadron collisions [30].

In considering hard exclusive processes, one needs to address the problem of the end point contributions – the so called Feynman mechanism. We find that due to the color neutrality of the pion and the effect of target recoil, the amplitude for this mechanism is suppressed by a factor $\propto 1/\kappa^2$ as compared with that of the perturbative QCD mechanism. The contribution of the Feynman mechanism is also suppressed by powers of the Sudakov-type form factor and by the form factor w_2 .

In previous papers [5,17] we have emphasized that the amplitude we computed in 1993 is calculable using perturbative QCD. However, there are five other types of contributions which occur at the same order of α_s . The previous term in which the interaction with the target gluons follows the gluon-exchange in the pion wave function has been denoted by T_1 . However, the two gluons from the nuclear target can also be annihilated by the exchanged gluon (color current of the pion wave function). This group of amplitudes is denoted as T_2 . Another term in which the interaction with the target gluons occur before the gluon-exchange in the wave function of dijet has been denoted by T_3 . There are also terms, denoted as T_4 , in which the interaction with the target gluons spans the entire time between interactions with target gluons. This term corresponds to the interaction of the $q\bar{q}g$ configuration with target gluons. Still another amplitude, T_5 , describes the interaction of $q\bar{q}$ dipole with a target in non-leading order in $\alpha_s \ln \kappa_t^2/\Lambda_{QCD}^2$.

Here is an outline of the remainder of this paper. Sect. II considers the κ_t^2 dependence of the Feynman diagrams and selects Feynman diagrams having the minimal power of $1/\kappa_t^2$ at fixed values of $\alpha_s \ln \kappa_t^2/\Lambda_{QCD}^2$ in the lowest order in α_s . We found that the processes where small size $q\bar{q}$ configuration is prepared before the scattering dominate diffractive dijet production. Subtle features of the arguments are discussed in Sect. III, which is concerned with the role of selection of exclusive processes in the suppressing of the contribution of hard processes related to inter-quark transverse distances $\gg 1/\kappa_t$. All of the terms T_{2-5} are shown to be negligible in the sense that they are smaller than T_1 by at least a power of α_s or by a factor of $\frac{\Lambda^2}{\kappa_t^2}$, or by powers of Sudakov-type form factors and/or of a form factor w_2 , which is related to the probability of finding a normal-sized $q\bar{q}$ configuration of the pion. At the end of this section we demonstrate that the contribution to high κ_t dijet production resulting from the scattering of a large size $q\bar{q}$ dipole by a large transverse momentum ($\approx \kappa_t$) component of the target gluon field is suppressed at least by two powers of the Sudakov-type form factor and by the w_2 form factor. Together sections II and III form the proof of the QCD factorization theorem for the diffractive dijet production. Rather general arguments for the small nature of the amplitudes T_{2-5} provided in the Sects. II and III are valid for the case of the photon projectile as well. This is because the contribution into the forward scattering amplitude of dijet production due to direct photon coupling to light quarks is \propto bare mass of quark and therefore small [31,32]. In the case of a charm quark photoproduction, the dominant term is given by a charm component of the direct photon wave function.

Sect. IV is concerned with the evaluation of the dominant amplitude T_1 , which has the form of the QCD factorization theorem in the leading order in α_s and all orders in $\alpha_s \ln(\kappa_t^2 r_\pi^2)$. The analysis performed in Sections II-IV shows that the z dependence of the leading (over powers of k_t^2) term in the amplitude of diffractive dijet production is given basically by the factor $z(1-z)$. The nuclear dependence of the amplitude, including a reassessment of the multiple-scattering correction of [5], and nuclear shadowing effects is discussed in Sect. V. Experimental aspects, including the requirements for observing color transparency and the extraction of the coherent cross section, are discussed in Sect. VI. There is an electromagnetic background term, which becomes increasingly more important as κ_t increases, in which the exchange of a photon with the target is responsible for the diffractive dissociation of the pion. This process, which occurs on the nuclear periphery and is therefore automatically free of initial and final state interactions, is shown in Sect. VII to provide a correction of less than a few percent contribution to the cross section at values of κ_t, s of the experiment [14] but this correction rapidly decreases with an increase in the value of κ_t . A discussion of the implications of observing color transparency as well as a summary and assessment of the present work is provided in the final Sect. VIII.

II. SELECTION OF DOMINANT FEYNMAN DIAGRAMS FOR $\pi N \rightarrow NJJ$ IN THE LEADING ORDER OF α_S AND $1/\kappa_T^2$

The kinematic constraints due to the energy-momentum conservation play an important role in the evaluation of amplitudes of diffractive processes. Therefore, we begin by deducing the necessary kinematical relations and introducing the light cone variables we use. Our interest is in the scattering at nearly forward angles. We denote momentum of the pion as p_π , and that of the target as p . The three momentum of the nucleus in the final state is $p_{fz} \approx M_{2jet}^2/2E_\pi = m_N x$. The first relation is expressed in terms of the variables of the nuclear rest frame, and the second is in the variables of IMF of a nucleus where $x = M_{2jet}^2/\nu$. The mass of the two jet system is given by $M_{2jet}^2 = \frac{m_q^2 + \kappa_t^2}{z(1-z)} \approx \kappa_t^2/z(1-z)$. We neglect the mass of quark m_q as compared with the large jet momentum κ_t . The quantity $\nu = 2(p_\pi p)/A$ is the invariant energy of collision. Our notation is that z represents the fraction of the total longitudinal momentum of the beam pion carried by the quark in the final state, and $1-z$ the fraction carried by the anti-quark. The transverse momenta are given by $\vec{\kappa}_t$ and $-\vec{\kappa}_t$. A is the number of nucleons in the nuclear target. Our interest is in the kinematics for which the final state nucleus remains intact. This means that minimal momentum transferred to nuclear target $-t_{min} \approx p_{f,z}^2$ should be small: $-t_{min} R_A^2/3 \ll 1$ i.e. $x \ll \frac{\sqrt{3}}{m_N R_A} \approx A^{-1/3}/3$. Here $R_A = 1.1A^{1/3}$ Fm is the nuclear radius. For small values of $-t_{min} R_A^2/3$, the effect of t_{min} can be easily accounted for because any form factor of the target can be approximated as $\exp tR_A^2/6$.

For large enough values of κ_t , the result of the calculations can be represented in a form in which only the $q\bar{q}$ components of the initial pion and final state wave functions are relevant in Eq. (42). See also the discussion at the beginning of section III. This is because we are considering a coherent nuclear process which leads to a final state consisting of a quark and anti-quark moving at high relative transverse momentum. It is necessary to examine the various momentum scales that appear in this problem. The dominant non-perturbative component of the pion wave function carries relative momenta (conjugate to the transverse separation between the q and \bar{q}) of the order of $p_t \sim \frac{\pi/2}{\sqrt{2/3}(2r_\pi)} \approx 300$ MeV. This is much, much smaller than the final state transverse relative momenta, which must be greater than about 2 GeV, the minimal value required to experimentally define a jet. The immediate implication is that the non-perturbative pion wave function, which is approximately a Gaussian, cannot supply the necessary high relative momenta. These momenta can only arise from the exchange of a hard gluon, and this can be treated using perturbative QCD.

Restricting ourselves to Feynman diagrams having the leading power of s , κ_t^2 , α_s (at fixed $\alpha_s \ln \kappa_t^2/\Lambda_{QCD}^2$ and/or $\alpha_s \ln 1/x$) and using a normal non-perturbative wave function which rapidly decreases with increase of the constituent transverse momentum gives the possibility of regrouping the diagrams into blocks having a rather direct physical meaning:

$$\mathcal{M}(N) = (T_1 + T_2 + T_3 + T_4 + T_5) . \quad (10)$$

Here the dominant terms T_1 and T_{1b} of Figs. 1 and 2 represent a type of impulse approximation, and we shall examine them first. Next we evaluate the possible role of color flow - of the interaction of target gluons with with gluon exchanged between quarks in the pion wave function -amplitude T_2 . This amplitude is also expressed through the same pion wave function as T_1 . The term T_3 corresponds to the final state interaction between jets. This will be followed by the discussion of the physical meaning of the other terms T_4, T_5 and the explanation of their smallness. At this point and below we rely heavily on the fact that, if $\alpha_s \ll 1$ in the leading $\alpha_s \ln \kappa_t^2/\Lambda_{QCD}^2$ and/or $\alpha_s \ln 1/x$ approximation, the sum of dominant diagrams (but not each particular diagram) has a ladder structure. In particular, various crossed diagrams which have a different form are needed to guarantee local gauge invariance for processes with large rapidity gaps, and to ensure the ladder structure of the sum of dominant diagrams. To derive such a ladder structure of the sum, it is important to explore crossing symmetry and the positive charge parity which follows from the dominance of the t-channel exchange two-gluon state of vacuum quantum numbers. Accurate exploring of gauge invariance is necessary for proving the ladder structure of the sum of Feynman diagrams. This structure makes it possible to include terms varying as $\ln 1/x$ and $\ln \kappa_t^2/\Lambda_{QCD}^2$, related to conventional QCD evolution, in skewed parton distributions or in skewed unintegrated gluon densities. In addition, we need to calculate the evolution of the pion wave function with transverse momentum and the interaction of gluons with this wave function. So we shall first classify and calculate skeleton diagrams, and then account for the QCD evolution.

A. Dimensional estimate of the initial state hard interaction

In our previous papers we investigated the term T_1 of Fig. 1. QCD is a non-Abelian gauge theory in which an exchanged gluon may probe the flow of color within the pion wave function. So in the leading order of α_s ,

the requirements of gauge invariance mandates that we should consider also the related set of diagrams where an exchanged gluon is attached to the exchanged gluon in the $q\bar{q}$ component of the pion wave function, see Fig 2.

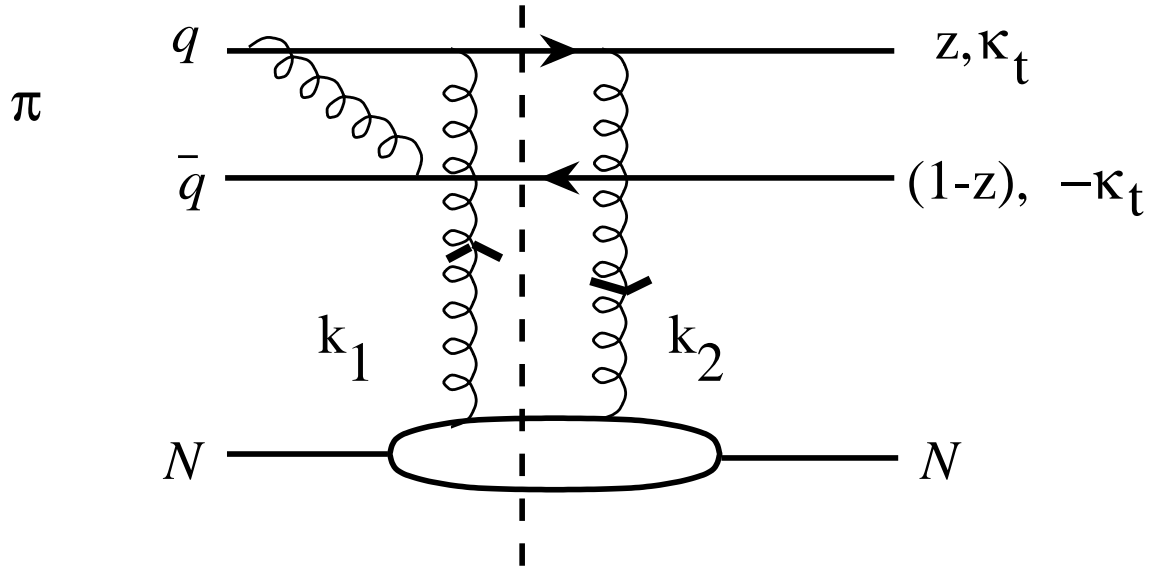


FIG. 1. A contribution to T_{1a} . The high momentum component of the pion interacts with the two-gluon field of the target. The displayed diagram occurs along with its version in which the gluons are crossed. Furthermore, there are four diagrams for each term because each of the gluons can be absorbed or emitted by either the quark or anti-quark of the beam pion. Thus only a single diagram of the eight that contribute is shown.

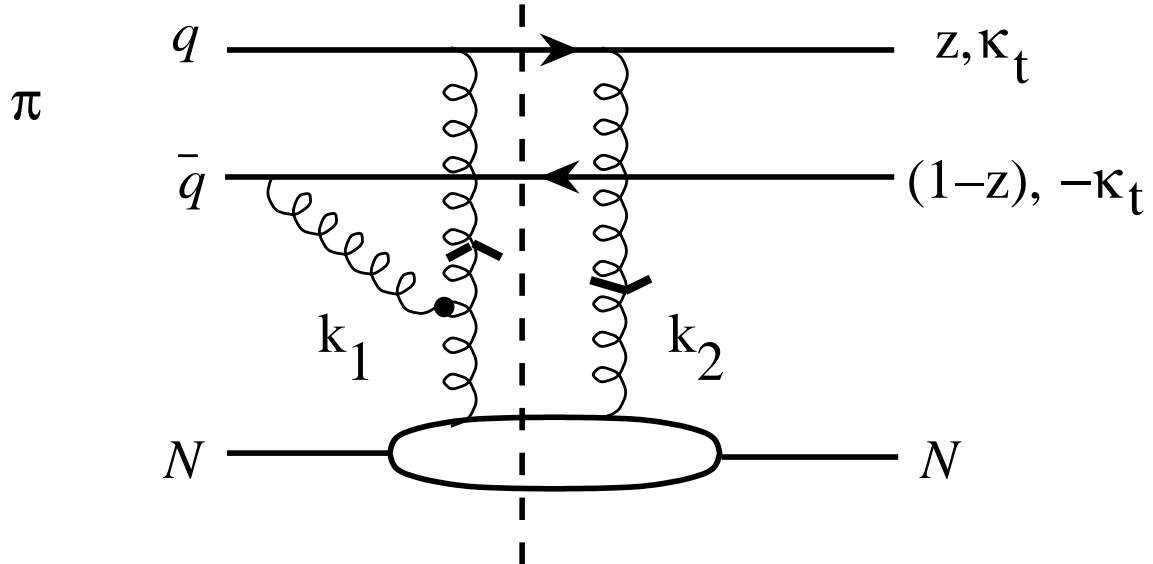


FIG. 2. A contribution to T_{1b} . The high momentum gluon current in the the pion wave function interacts with the two-gluon field of the target. The displayed diagram occurs along with its version in which the gluons are crossed, for different attachments of gluons in the pion wave function. Thus only a single diagram of the eight that contributes is shown.

In the evaluation of the terms of Figs. 1 and 2, with color flow we use Gribov's observation [6] that, within the leading $\alpha_s \ln 1/x$ approximation, the polarization of gluons exchanged in the ladder is $\propto p$ where p is the four momentum of

the target. It is not difficult to show that the same gluon polarization dominates in the calculation of QCD evolution in the leading order in $\ln \kappa_t^2 / \Lambda_{QCD}^2$. It is also convenient to use the fact that only one gluon is off its mass shell (in the leading logarithmic approximation considered in the paper). This causes the equation that describes the conservation of color current to have the same form as in QED. We show here that the use of QED-type Ward identities [28] (allowed in computing the s, u cuts of the diagram, as explained in the Introduction) leads to the result that only the transverse components of the gluon momenta k_1, k_2 enter in the final result for the amplitudes T_{1a}, T_{1b} . Momentum factors, related to the contribution of the target gluons, are included by definition in the skewed gluon distribution.

We examine the part of T_{1a}, T_{1b} that arises from the exchange of the gluon k_1 and that gives an on-shell $q\bar{q}$ intermediate state. The result is

$$T_1 = T_{1a} + T_{1b} \propto A_{\mu\nu}^{\pi} d^{\mu\nu} d^{\bar{\mu}\bar{\nu}} A_{\bar{\mu}\bar{\nu}}^N \dots, \quad (11)$$

where $A^{\pi, N}$ represents the gluon emission amplitude of the pion, nucleon and $d^{\mu\nu}$ arising from the propagator of the gluons emitted or absorbed by the target. At high energies, the gluon propagator can be represented as [6]

$$d^{\mu\nu} \propto \frac{2p^{\mu} p_{\pi}^{\nu}}{2p_{\pi} \cdot p}, \quad (12)$$

where p^{μ} is the nucleon momentum, so that

$$T_{1a} + T_{1b} \propto \frac{2A_{\mu\lambda}^{\pi} p_{\mu} p_{\lambda}}{2p_{\pi} \cdot p} \frac{2A_{\bar{\mu}\bar{\nu}}^N p_{\bar{\mu}}^{\pi} p_{\bar{\nu}}^{\pi}}{2p_{\pi} \cdot p}. \quad (13)$$

We will denote this presentation of the contribution of gluon exchanges-as the Gribov representation because he was the first to understand the dominance in the high energy processes of gluon polarization $\propto p$, see [6]. Now we use current conservation,

$$A_{\mu\lambda}^{\pi} \cdot k_{1\mu} = 0, \quad (14)$$

and employ Sudakov variables to describe the momentum k_1 :

$$k_1^{\mu} = x_1 p^{\mu} + \beta p_{\pi}^{\nu} + k_t. \quad (15)$$

We can determine the quantities α, β by taking the dot product of the above equation with either p or p_{π} and neglecting the relatively small factors of the square of the pion or nucleon mass. This gives

$$\begin{aligned} x_1 &= \frac{k_1 \cdot p_{\pi}}{p \cdot p_{\pi}}, \\ \beta &= \frac{\kappa_1 \cdot p}{p \cdot p_{\pi}}. \end{aligned} \quad (16)$$

Using these results in the current conservation relation (14) leads to the relation:

$$A_{\mu\lambda}^{\pi} \cdot p_{\mu} = -\frac{\beta}{x_1} A_{\mu\lambda}^{\pi} \cdot p_{\pi} - \frac{A_{\mu\lambda}^{\pi} \cdot \kappa_{1t\mu}}{x_1}. \quad (17)$$

The first and third terms of Eq. (17), in difference from the second, are proportional to s and therefore dominate over the second [6]. Thus we find

$$A_{\mu\lambda}^{\pi} \cdot p_{\mu} \approx -\frac{A_{\mu\lambda}^{\pi} \cdot \kappa_{1t\mu}}{x_1}, \quad (18)$$

so that the exchange of the gluon k_1 gives an amplitude (13) proportional to the small transverse momentum κ_{1t} . The net result of these considerations is that the contribution of the gauge invariant set of the diagrams including those of Figs 1, 2 takes the form:

$$T_{1a} + T_{1b} \propto \frac{2A_{\mu\lambda}^{\pi} \cdot k_{1\mu} p_{\lambda}}{(2k_1 \cdot p_{\pi})} \dots \frac{2A_{\mu'\lambda'}^N \cdot p_{\mu'}^{\pi} p_{\lambda'}^{\pi}}{(2p_{\pi} \cdot p)}. \quad (19)$$

The same trick can be made with the second exchanged gluon:

$$T_{1a} + T_{1b} \propto \frac{4A_{\mu\lambda}^{\pi} \cdot k_{1\mu} k_{2\lambda t}}{(2k_1 \cdot p_{\pi})(2k_2 \cdot p_{\pi})} \cdots A_{\mu'\lambda'}^N \cdot p_{\mu'}^{\pi} p_{\lambda'}^{\pi}. \quad (20)$$

The factors involving k_{it} will be absorbed into the definition of the skewed gluon distribution of the nucleon. The useful result is in the denominator of Eqs. (19,20), because

$$2k_i \cdot p = x_i s. \quad (21)$$

So

$$T_{1a} + T_{1b} \propto \frac{4A_{\mu\lambda}^{\pi} \cdot k_{1\mu} k_{2\lambda t}}{(x_1\nu)(x_2\nu)} \cdots A_{\mu'\lambda'}^N \cdot p_{\mu'}^{\pi} p_{\lambda'}^{\pi}. \quad (22)$$

This formula in which the amplitude is expressed in terms of exchanges by transversely polarized gluons is the adjustment to QCD of the Weizsacker-Williams (WW) method of equivalent photons [33], of the Gribov derivation of reggeon calculus [6], and of the Cheng & Wu's impact parameter representation [34]. So below we will denote such a formula as the Weizsacker-Williams representation of equivalent gluons. For the calculation of the dominant amplitude T_1 , such a trick is not very useful because effectively $x_2 \ll x_1$. So in this case we shall use the Gribov representation for the second exchanged gluon.

Let us first perform power counting for the sum of terms $T_{1a} + T_{1b}$ within the Gribov representation for the amplitude. The number of strongly virtual propagators in Fig 1 is two and the number of large transverse momenta in the numerator from the vertexes is two. An additional factor $1/\kappa_t^2$ follows from the cancellation of the sum of leading diagrams because of the color neutrality of the pion. In the following we include the factor α_s/κ_t^2 as part of the high momentum component of pion wave function. Slowly changing factors such as $\alpha_s, \ln x, \ln(\kappa^2/\Lambda_{QCD}^2)$ are included by definition in the skewed gluon distribution xG_A and into the pion wave function. Finally we obtain: $T_{1a} \propto \alpha_s \chi_{\pi}(z, \kappa_t^2) x_1 G_A(x_1, x_2, \kappa_t^2)/\kappa_t^2$. This result can be easily proved within the WW representation also. Note also that the comparison of the above result with the WW representation shows that the kinematical region around $x_2 \approx 0$ gives a negligible contribution to the integral over k_{it}, β, x_1 .

The contribution of the color exchange current - the term T_{1b} - is suppressed in the light-cone gauge as compared to T_{1a} by a power of κ_t . To estimate the k_t dependence of the diagrams, we shall use the WW representation of the gluon exchange between quarks in the initial pion and the target and the Gribov representation for gluon exchange with the target in the final state. Within this representation for the sum of diagrams, the cancellation between diagrams leading to the number of powers of $\frac{1}{\kappa_t^2}$ is accounted for in a straightforward way. So the contribution of energy denominators gives: $\frac{1}{(\kappa_t^2)^3}$. Additional $\frac{1}{x_1\nu} \propto \frac{1}{k_t^2}$ as compared to the product of gluon propagators is a result of cancellations between diagrams due to color neutrality of pion and final state of two jets. Account of gluon momenta in the nominator gives 0 when both gluons in the gluon color current in the pion wave function are longitudinally polarized: $(k_{1t})_r p_{\mu, \pi} p_{\lambda, \pi} g_{\mu, \lambda}^r = 0$. The contribution in the denominator when one of the gluons in the gluon color current in the pion wave function is longitudinally polarized, while the second is transversely polarized, also vanishes. This is because forward scattering cannot change helicity. The proof of this statement follows from the combination of the light cone gauge condition: $A_- = 0$ and the fact that the leading power of s is given by the $+$ vertex for the interaction of a nuclear gluon with a quark. Accounting for the color neutrality of the pion wave function and of the wave function of the dijet final state, as well as the anti-symmetry of 3 gluon vertex is also important.

The use of identity: $(k_{1t})_r \kappa_{\mu, t} \kappa_{\lambda, t} g_{\mu, \lambda}^r = 0$ helps to prove that the leading contribution into T_{1b} is 0 when both gluons in the gluon color current in the pion wave function are transversely polarized. Here k_{1t} is the transverse momentum of a gluon exchanged with target and κ_t is the transverse momentum of the jet. $g_{\mu, \lambda}^r$ is the Yang-Mills three-gluon vertex.

The physical meaning of the obtained result for $T_{1a} + T_{1b}$ is that the interaction of quarks in the pion wave function with the target gluon with a relatively low virtuality is dominated by distances significantly larger than that involved in the pion wave function, and by the target gluon interaction with external lines of the amplitude without a gluon. This is the generalization to QCD of a theorem proved for QED by Low [35].

For completeness we present the result of the calculation of Feynman diagrams for T_1 in the leading $\alpha_s \ln \frac{\kappa_t^2}{\Lambda_{QCD}^2}$ approximation where the integration over fraction of pion momentum β transferred to the target gluon by quarks in the pion wave function is not performed. The derivation is rather close to that in [36] because in the leading $\alpha_s \ln \frac{\kappa_t^2}{\Lambda_{QCD}^2}$ approximation the same polarization of target gluons dominates as in the leading $\alpha_s \ln 1/x$ approximation. The deduced formula is actually very similar to the formula deduced in [36] for hard diffractive vector meson production where in the leading $\ln 1/x$ approximation the integral over the unintegrated gluon density is replaced in the final step by the gluon density. So we will not repeat the detailed evaluation made in [36].

The result is:

$$T_1/\nu = \int \alpha_s (2(2\chi(z, k_t^2) - \chi(z + \beta, k_t^2) - \chi(z - \beta, k_t^2)) + \Delta(\chi(z + \beta, k_t^2) + \chi(z - \beta, k_t^2))) \cdot \frac{1}{d_f(\kappa_t^2)} \frac{k_{1t}^2}{2} F^2(3) \pi^2 \frac{d\beta}{\beta} d^2 k_{1t} \frac{f_T}{k_1^2 k_2^2}. \quad (23)$$

Here Δ is the two dimensional k_t space Laplacian operator which acts on the pion wave function, $f_T = \frac{A_{\mu,\lambda}^T k_{1t,\mu} k_{1t,\lambda}}{\beta\nu(2\pi)^4}$. The first term of Eq. (23) is small and we shall explain why we neglect it. The factor: $\frac{1}{d_f(\kappa_t^2)}$ follows from the definition of the pion wave function and from the definition of hard amplitude in terms of series over the powers of the running coupling constant. The amplitude T_1 can be simplified by using the leading $\ln 1/x$ approximation. In particular, one may express the amplitude in terms of the gluon distribution [36]. This gluon distribution is however different from the usual gluon distribution determined from DIS processes because of the significant difference between the masses of the initial pion and final two jet systems. The necessary skewed gluon distribution is calculable for small values of x as the solution of QCD evolution equation, using the ordinary diagonal gluon distribution as the initial condition [11]. Here, in a fashion similar to [36], we approximate: $xG = \int d^2 k_{1t} \frac{k_{1t}^2}{k_1^2 k_2^2} \int_{\beta_0}^1 \frac{d\beta}{\beta} f_T$, so that f_T can be denoted the unintegrated gluon density. Equation (23) is a version of Eq. (1), in which the dipole approximation (keeping terms of the order r_t^2 in the bracket $[2 - \exp(-i(\mathbf{r}_t \cdot \mathbf{k}_{1t})) - \exp(i(\mathbf{r}_t \cdot \mathbf{k}_{1t}))]$ in Eq. (1)) is used. This approximation is reasonable even if $(k_{it} r_t)$ is comparable or even larger than 1 (cf. discussion in [36] after Eq. (2.20)). Another useful approximation involves the value of β appearing in the argument of the pion wave function. The upper limit of integration over β is dictated by energy conservation to be $\beta \leq 1$. For $z \sim 1$ one gets a further restriction that $\beta \leq 1 - z$. But in the leading $\log \frac{\kappa_t^2}{\Lambda_{QCD}^2}$ approximation, the condition for the region of integration in β is more severe. It is given by the requirement that the contribution of the target gluon longitudinal momentum into its propagator $\approx \beta M_{2jet}^2$ should satisfy conditions: $\beta M_{2jet}^2 \approx k_{1t}^2 \ll M_{2jet}^2$. Hence in Eq.(23) it is legitimate to neglect β in the argument of the pion wave function, and to keep in Eq.(23) the term $\propto \Delta$ only. The value of the lower limit of the integration: $\beta \geq \beta_0$ is obtained from the energy conservation law, and from the QCD evolution which effectively suppresses the contribution of the region $k_1^2/\beta_0\nu \sim 1$.

Elastic interactions between high κ_t q and \bar{q} in the final state may lead to an infrared contribution which is exactly canceled in the probability summed over the final state gluon radiation. It is important that the complete nature of final states allows the term T_1 to account for the final state radiation and the space-time evolution of the $q\bar{q}$ pair in the final state. This phenomenon is a familiar feature of the theoretical analysis of the fragmentation of the small size wave packet, of $e + \bar{e} \rightarrow hadrons$.

B. Meson Color Flow Term— T_2

The T_2 or meson-color-flow term, of Fig. 3 arises from the $q\bar{q}g$ intermediate state, or from the attachment of both target gluons to the exchanged gluon or to the exchanged gluon and the quark(anti-quark).

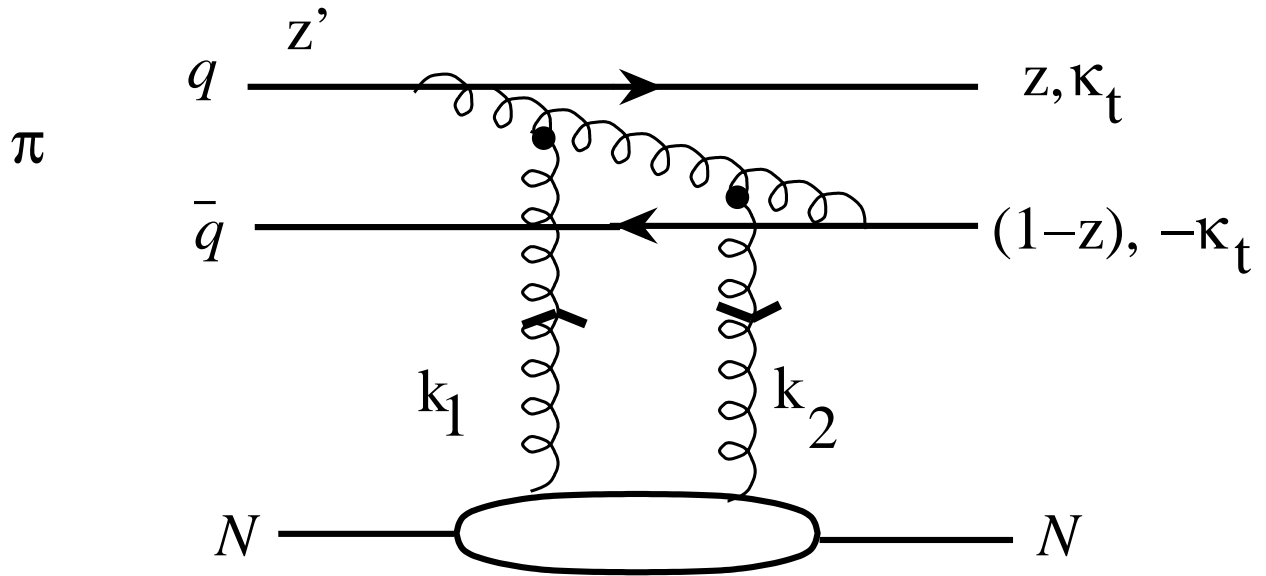


FIG. 3. Contribution to T_{2a} of $q\bar{q}g$ intermediate state. The exchanged gluon interacts with each of the target gluons. There is also a diagram in which the gluons from the target are crossed, and another two in which the exchanged gluon is emitted by the anti-quark. Only a single diagram of the four that contribute is shown.

The diagrams of Fig. 3, considered in this section, have the same topology as the diagrams included in the term T_1 and therefore have the same power of $\frac{\Lambda_{QCD}^2}{\kappa_t^2}$, and $\ln 1/x$. In particular, they are included in T_1 if $l_t^2 \ll \kappa_t^2$. (To visualize the relationship between T_1 and T_2 it is useful to move down the point of attachment of target gluons to the gluon in the pion wave function in the diagram Fig. 3.) In this case, a significant contribution may arise only from the perturbative high momentum tail of the pion wave function. The effects of the gluon-gluon interaction may then be included as part of the target gluon distribution. In the case when the square of the transverse momenta of the gluon in the pion wave function is $\propto \kappa_t^2$, this diagram can be considered as a non-leading order correction (to the dipole-target interaction cross section) in α_s at fixed values of $\alpha_s \ln \frac{\kappa_t^2}{\Lambda_{QCD}^2}$. In contrast with the term T_2 , the definition of T_1 contains a requirement that the transverse momenta of gluons attached to quark lines should be much less than κ_t^2 , and that the pion wave function includes its perturbative tail. For the terms of Fig. 3, the non-perturbative pion wave function cuts off large quark momenta in the pion wave function. Thus gluonic transverse momenta are $\approx \kappa_t^2$, but transverse momenta of target gluons are still small: $\kappa_{t_i}^2 \ll \kappa_t^2$. The contributions of other diagrams with an almost on shell $q\bar{q}g$ intermediate state, see Fig. 4, are not suppressed by a power of $\frac{\Lambda_{QCD}^2}{\kappa_t^2}$.

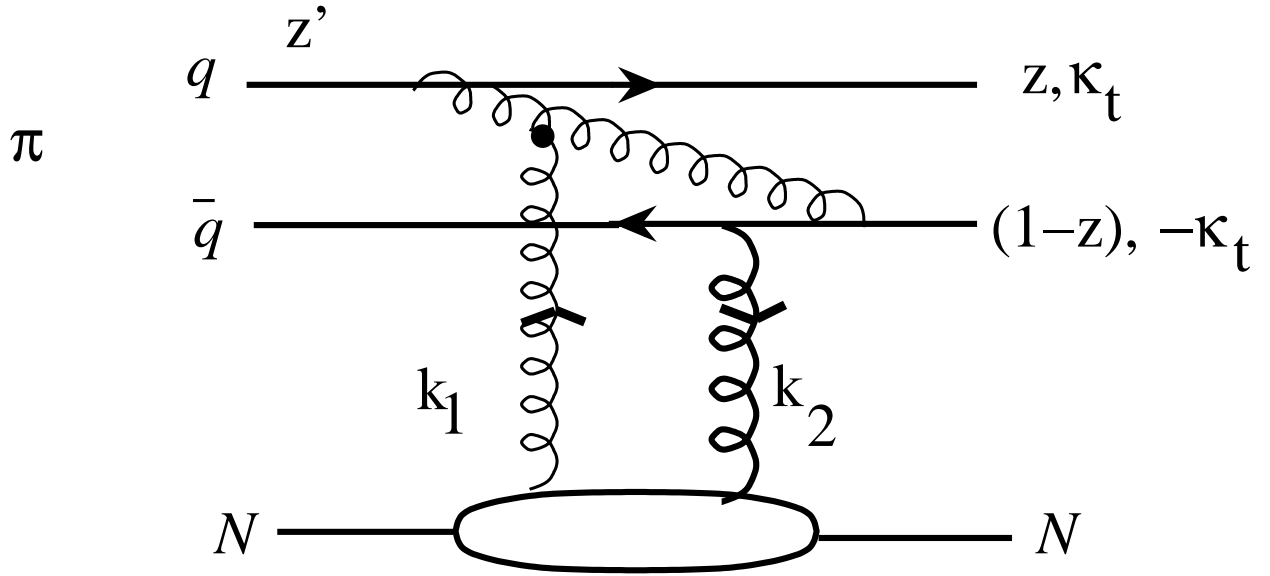


FIG. 4. Contribution to T_{2b} from $q\bar{q}g$ intermediate state. The interaction of one target gluon field with exchanged gluon in the intermediate states. There is also a diagram in which the gluons from the target are crossed, and another group in which the exchanged gluon is emitted by the anti-quark. Only one of 16 diagrams that contribute is shown.

It is easy to calculate the sum of the terms $T_{2a,2b}$ in the framework of the Gribov representation where dominant contribution is given by the polarization of a target gluon which is \propto target four momentum. Most straightforward calculation is for the ratio $\frac{T_2}{T_1}$ because in this ratio all factors except the z dependence are canceled out. Really quark-gluon vertexes when gluons are attached to quark(anti-quark) lines in the pion wave function are the same for the terms T_1, T_2 . In the light cone gauge all factors from the vertexes for the interaction of target gluons with a gluon in the initial and final state wave functions are effectively the same as for a gluon interaction with quarks except for the Casimir operator of the color group in the octet and the triplet representation. A subtle point of calculation is to evaluate the z dependence of this ratio. For certainty in the evaluation of term T_2 we assume that the nonperturbative pion wave function is equal to the asymptotic one.

Thus the ratio is determined by the color content of color flow in the pion wave function and the quark color and by the dependence of energy denominators on the fraction of pion momentum carried by quarks and gluons. So

$$\frac{T_2}{T_1} = \frac{F^2(8)}{F^2(3)} \left(-1 + \frac{1}{z(1-z)} + \frac{z}{(1-z)^2} \ln z + \frac{(1-z)}{z^2} \ln(1-z) \right) \quad (24)$$

Here $F^2(i)$ (for $i = 8, 3$ is the Casimir operator for octet and triplet representations of color group $SU(3)_c$. The ratio $\frac{T_2}{T_1}$ is ≈ 0.5 for $z = 1/2$, remains nearly constant for $|z - .5| \leq 0.3$ and increases to $9/8$ at $z=0,1$. This term is additionally suppressed by the Sudakov type form factor and by the form factor w_2 -see the discussion below.

C. Final state interaction of $q\bar{q}$ Pair- T_3

The interaction with the target gluons may occur before the interaction between quarks in the final state, and the related amplitudes are denoted as T_3 , see Figs. 5 and 6.

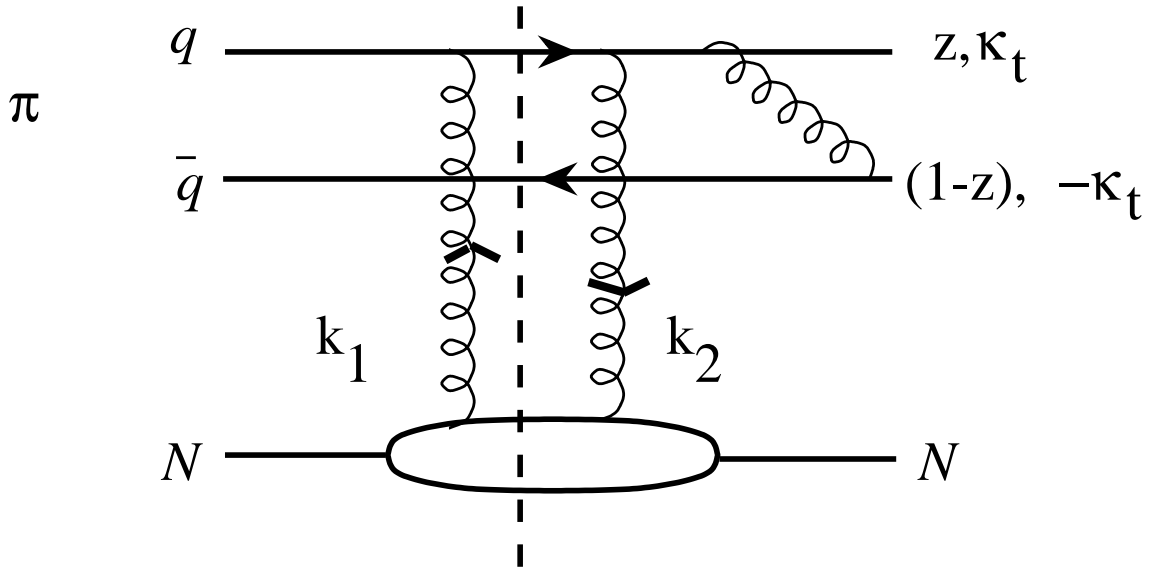


FIG. 5. Contribution to T_{3a} . The high momentum component of the final $q\bar{q}$ pair interacts with the two-gluon field of the target. Only a single diagram of the eight that contribute is shown.

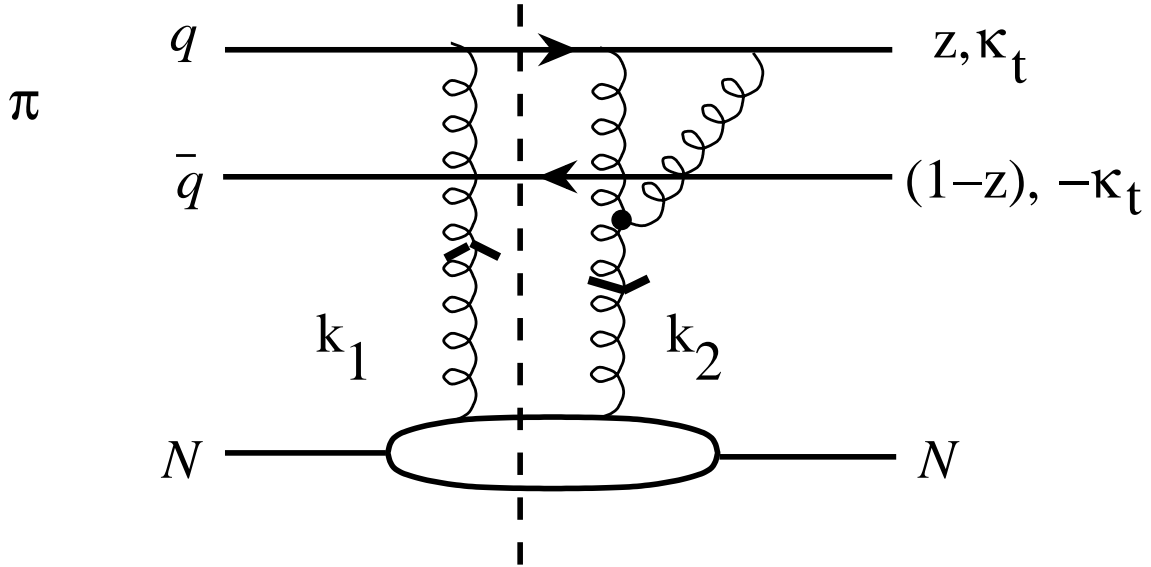


FIG. 6. Contribution to T_{3b} . The gluon from the two-gluon field of the target interacts with the high momentum component of the final $q\bar{q}$ pair wave function. Only a single diagram of the eight that contribute is shown.

The term T_{3a} includes the effect of the final state $q\bar{q}$ interaction. Fig. 6 includes the interaction of a target gluon with color flow in the wave function of final state.

We need to evaluate only the s -, u - channel cuts of the diagram (and use Eq. (4) to get any necessary real part). It is useful to define l_t as the quark transverse momentum within the pion wave function. Then there are two kinematic regimes to consider. The first has $l_t \ll \kappa_t$, $k_{1t} \ll \kappa_t$, and the second $l_t^2 \sim k_{1t}^2 \sim \kappa_t^2$. We consider the former regime first, as it is expected to be more important. In this case, we shall employ conservation of the four-momentum to evaluate x_2 . Conservation of the four-momentum can be used to relate the intermediate state (denoted by the vertical dashed line, occurring between the emission and the absorption of the gluons by the target in the diagram of Fig. 5

[37]) of momentum \tilde{p} with $\tilde{p}^2 \equiv \tilde{m}^2$ with the intermediate state. The mass of the $q\bar{q}$ intermediate state is given by

$$\tilde{m}^2 \approx x_1\nu - x_1\beta\nu - k_{1t}^2, \quad (25)$$

where β is the light-cone fraction of the pion momentum carried by an exchanged gluon: $\beta = \frac{-k_1^-}{p_\pi^-} = \frac{-k_2^-}{p_\pi^-}$. Thus we arrive at the equation:

$$x_1 = \frac{\tilde{m}^2 + k_{1t}^2}{(1-\beta)\nu}. \quad (26)$$

It follows from the requirement of positivity of energies of all produced particles in the intermediate states that $0 \leq \beta \leq 1$. We can now calculate \tilde{m}^2 directly in terms of the light cone momenta of the $q\bar{q}$ pair in the intermediate state:

$$\tilde{m}^2 = \left(\frac{l_t^2}{z} + \frac{(k_{1t} - l_t)^2}{1-z-\beta} \right) (1-\beta) - k_{1t}^2. \quad (27)$$

Combining Eqs. (25),(27) we obtain

$$\frac{l_t^2}{z} + \frac{(k_{1t} - l_t)^2}{1-\beta-z} = x_1\nu, \quad (28)$$

which, when using Eq. (6) leads to

$$x_1 = \frac{1}{\nu} \left(\frac{l_t^2}{z} + \frac{(k_{1t} - l_t)^2}{1-\beta-z} \right) = \frac{m_{2jet}^2}{\nu} + x_2, \quad (29)$$

Therefore

$$x_2 = \frac{1}{\nu} \left(\frac{l_t^2}{z} + \frac{(k_{1t} - l_t)^2}{1-\beta-z} - \frac{\kappa_t^2}{z(1-z)} \right). \quad (30)$$

In order for the term T_{3a} to compete with T_{1a} we need to have $l_t \ll \kappa_t$, $k_{1t} \ll \kappa_t$ -otherwise T_{3a} will be additionally suppressed by the power of κ_t^2, α_s . These kinematics cause Eq. (30) to yield the result: $-x_2 \propto \kappa_t^2/\nu$.

This argument can be carried out for all combinations of diagrams represented by Fig. 5. For example, another attachment of gluons, in which the gluon k_1 is absorbed by the quark, corresponds to interchanging z with $1-z$, and therefore leads to the same result for x_2 . Evidently this result for x_2 is valid in the leading $\alpha_s \ln \kappa_t^2/\Lambda_{QCD}^2$ approximation also. Thus we consider the second situation: $l_t^2 \sim k_{1t}^2 \sim \kappa_t^2$. In this case, the initial pion wave function contains a hard quark, and we discuss hard radiative correction in the next order of α_s . This is the typical situation in which there are extra hard lines, as compared with the dominant terms, and one obtains a suppression factor $\sim 1/\kappa_t^2$ which could be compensated by d^2k_t integral. However this integral does not produce $\ln \kappa_t^2/\Lambda_{QCD}^2$ because the region of integration is too narrow. So this contribution is at most NLO correction over α_s . But we restrict ourselves by the LO contribution only.

The presence of color flow in the wave function of the final state leads to the interaction of a target gluon with a gluon in the wave function of the final state, see Fig.6. This term is suppressed by an additional power of $1/\kappa_t^2$. The proof of this statement repeats the same reasoning as that explaining the suppression of the term T_{1b} . It heavily uses the WW and the Gribov representations, discussed in subsection A, and the identities which follow from the antisymmetry of the vertex for the three gluon interaction, the color neutrality of the pion wave function, and the dijet final state. In the derivation it is helpful to use the observation that effectively $|x_2| \propto \kappa_t^2/\nu$. Evidently similar reasoning is applicable in computing amplitudes to leading order in α_s and all orders in $\alpha_s \ln \kappa_t^2/l_t^2$.

Repeating the same reasoning as in the estimate of the terms of T_{1a}, T_{1b} , and remembering that $-x_2 \approx \kappa_t^2/\nu$ we achieve the estimate: $T_3 \propto \alpha_s^2 x_1 G_A(x_1, x_2, \kappa_t^2)/\kappa_t^4$. It is instructive to investigate whether the Feynman mechanism, where the leading quark (anti-quark) carries a fraction of the pion momentum z' close to 1 but high momentum jets are formed by the action of a final state interaction, may compete with the PQCD description. In this case transverse momenta of constituents l_t in the pion wave function are expected to be equal to the mean transverse momenta of partons in the non-perturbative regime. For certainty let us model the Feynman mechanism by assuming that recoil system is quark(anti-quark) with momentum $1-z'$ close to 0. Within this model we will obtain Feynman diagrams for the term T_2 , but with the region of integration defined by the Feynman mechanism. A simple dimensional evaluation of term T_3 due to the Feynman mechanism within the Gribov representation shows that it is suppressed by the

powers of κ_t . The contribution of the region $\frac{l_t^2}{(1-z')} \ll M_{2jet}^2$ has been considered above-it is additionally suppressed for Feynman mechanism by the restriction of the region of integration over z' . Thus our next discussion is restricted by the consideration of the contribution of the region: $\frac{l_t^2}{(1-z')} \geq M_{2jet}^2$.

$$T_3 \propto \frac{1}{\kappa_t^2} \int \psi_\pi(z', l_t^2) \frac{1}{M_{int}^2 - M_{2jet}^2} \frac{(l_t)^2}{(1-z')} d^2 l_t dz' \quad (31)$$

In the above formulae we use Brodsky-Lepage convention for the definition of wave functions and retain terms maximally singular when $z' \rightarrow 1$. Power counting is simple: the factor $\frac{l_t^2}{(1-z')\kappa_t^2}$ is from the gluon exchange in the final state. The factor $l_t^2/(1-z')$ is singular when $z' \rightarrow 1$. It originates from the quark vertexes accompanying the propagator of the gluon exchanged in the wave function of final state. Here $1/(1-z')$ follows from a transition when a fraction of the pion momentum carried by quark tends to 0. The factor $M^2(2jet) - l_t^2/z'(1-z')$ in the denominator is due the fermion propagator adjacent to the hard gluon exchange in the wave function of the final state. Here $M_{int}^2 \approx \frac{m_{rec}^2 + l_t^2}{1-z'}$ is the mass of an intermediate state, and m_{rec}^2 is the invariant mass of the recoil system in the Feynman mechanism. In the region of integration $1-z' \ll l_t^2/M_{2jet}^2$ one may neglect by $M^2(2jet)$ in the denominator as compared to $l_t^2/(1-z')$. So one obtains : $T_2 \propto \frac{1}{\kappa_t^2} \int \psi_\pi(z', l_t^2) d^2 l_t dz'$. In this case, another factor of $1/\kappa_t^4$ arises from the integration over z' . Hence we have found that the Feynman mechanism is a higher twist correction to the PQCD contribution. The Feynman mechanism is further suppressed by the requirement of a lack of collinear to pion momentum radiation-see the discussion below.

D. Gluon admixture to the wave functions of initial and final states - T_4

The Feynman diagram corresponding to Fig. 7 contains the time ordering corresponding to the $q\bar{q}g$ configuration in the pion wave function interacting with the quarks in the final state. In taking the imaginary part of the amplitude, the intermediate state must contain a hard on-shell quark and a hard on-shell gluon. But such a state cannot be produced by a soft almost on-shell quark in the initial state, so there is an additional suppression factor, caused by the rapid decrease of the non-perturbative pion wave function with increasing quark virtuality. This factor is greater than a power of κ_t^2 . One may also consider the case when the transverse momenta of quarks in the pion wave function are large enough to use PQCD. Then the large virtuality of the quark introduces a suppression factor of $\frac{1}{\kappa_t^2 l_t^2}$, with at least one power of $\frac{1}{\kappa_t^2}$ arising from the quark line for the transition $q \rightarrow qg$ and another factor of $\frac{1}{l_t^2}$ arising from the pion wave function. There are additional factors: $\frac{1}{\kappa_t^2}$ arises from the hard fermion line, and $\frac{1}{\kappa_t^4}$ from the application of Ward identities and the condition: $x_1\nu, x_2\nu \propto \kappa_t^2$. A factor of $\kappa_t^2 l_t^2$ is present in the numerator, with κ_t^2 originating from the vertices in the WW representation and l_t^2 from the integration over quark momenta in the pion wave function. All in all this amplitude is suppressed by the factor $l_t^2/(\kappa_t^2)^3$. Another case occurs when $l_t^2 \propto \kappa_t^2$. Then this diagram will be suppressed as compared to T_1 at least by one power of α_s without the large factor $\ln \kappa_t^2/\Lambda_{QCD}^2$. But here we restrict ourselves to the analysis of LO corrections.

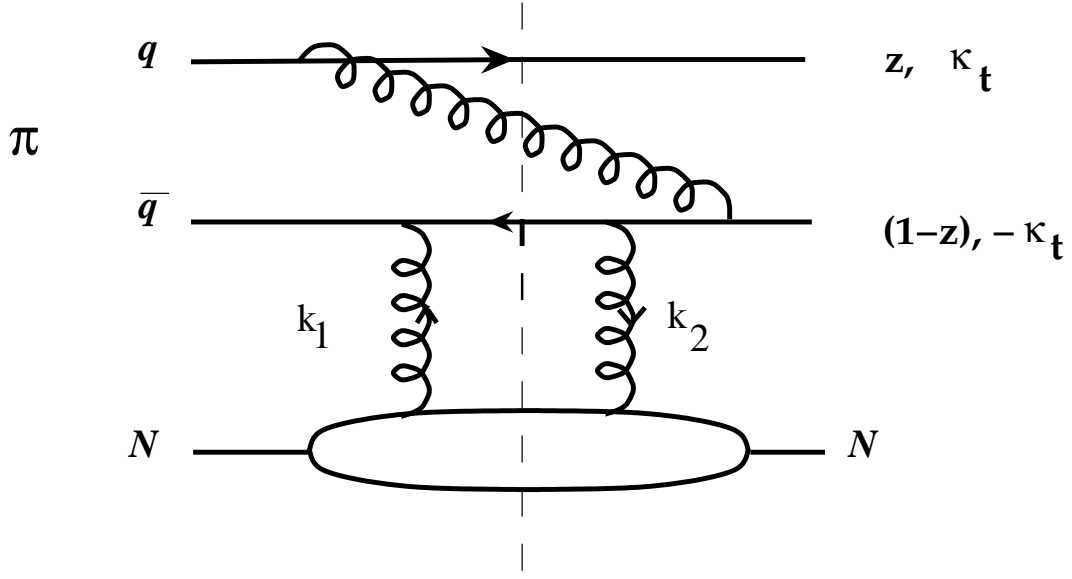


FIG. 7. A time ordering that contributes to T_4 . The $q\bar{q}g$ state interacts with the target. Only a single diagram of the eight where a gluon interacts with quarks in a pion fragmentation region that contribute is shown.

Similar reasoning helps to prove that the contribution of diagrams in Fig. 6 is suppressed by a factor l_t^2/κ_t^2 as compared to that in Fig. 1. This is the power-type suppression if the pion wave function is non-perturbative, and may be a NLO α_s correction if the perturbative high momentum tail is included in the pion wave function.

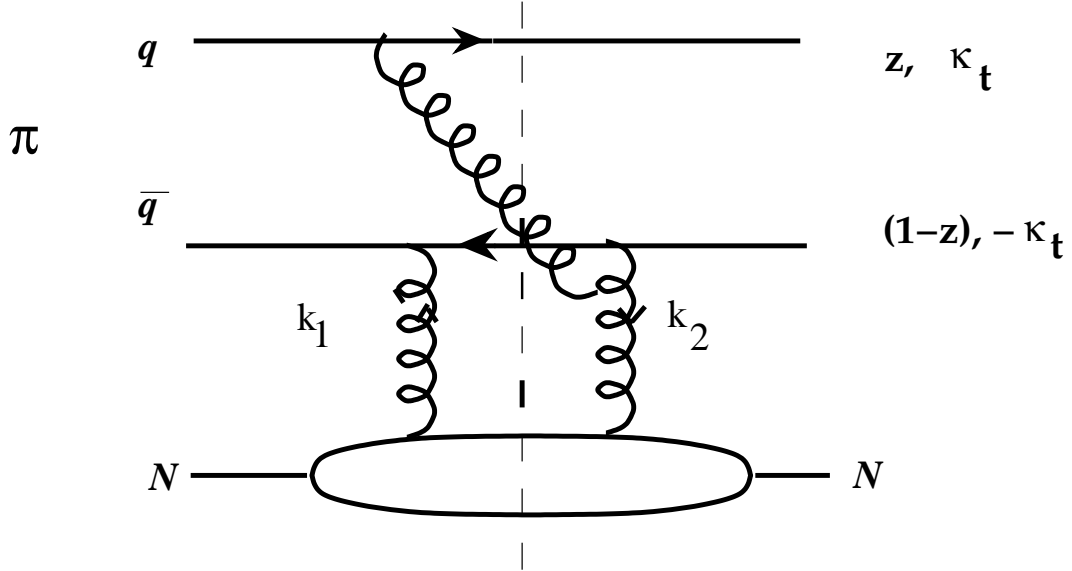


FIG. 8. A contribution to T_{4b} . The target gluon absorbs a gluon of pion wave function. Only one diagram of the eight that occur is shown.

Another contribution to T_4 arises from the sum of Feynman diagrams in which the gluon exchange between the q and \bar{q} in the beam occurs during the interaction with the target, see Figs. 8, 9, and 10. The naive expectation is that such terms, which amount to having a gluon exchanged during the very short interaction time characteristic of the two gluon exchange process occurring at high energies, must be very small indeed.

The intent of this sub-section is to use the analytic properties of the scattering amplitude to show that T_4 is

negligible. Instead of calculating the sum of the imaginary parts of all of the amplitudes, we will prove that this sum vanishes by analyzing analytic properties of the important diagrams. Each considered diagram contains a product of an intermediate-state quark and anti-quark propagator. At high energies, these propagators are controlled by the terms of highest power of x_1 $2p \cdot p_\pi = x_1 \nu$, and (as to be shown) have poles in the complex x_1 plane which are located on one side of the contour of integration. The sign of the term containing (ν) in each propagator unambiguously follows from the directions of pion and target momenta. If we can show that the typical integral is of the form

$$\int dx_1 \frac{1}{(\alpha x_1 \nu - a + i\epsilon)(\beta x_1 \nu - b + i\epsilon)}, \quad \alpha, \beta > 0 \quad (32)$$

the proof would be complete.

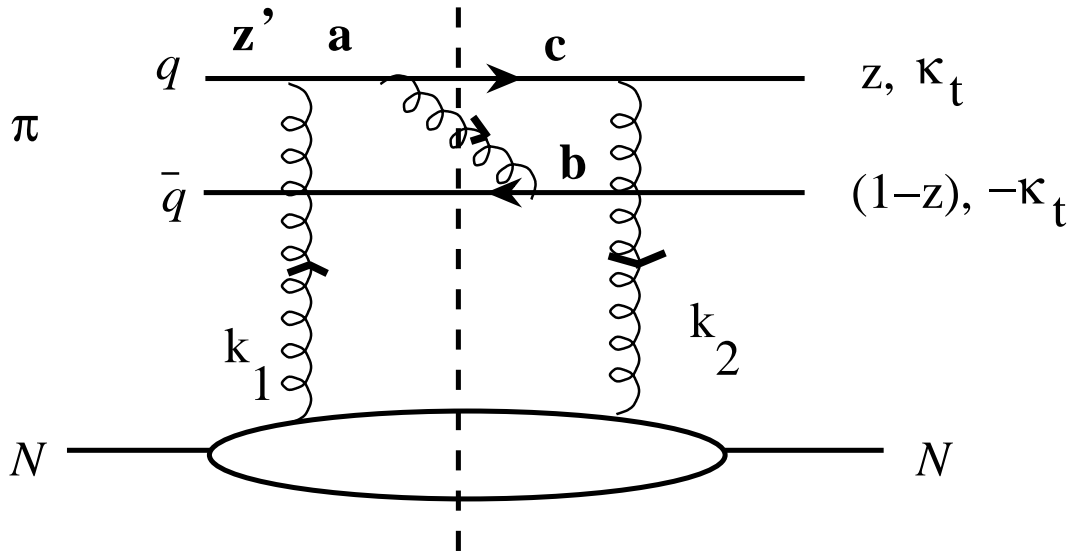


FIG. 9. A contribution to T_{4c} . The quark absorbs a gluon of momentum k_1 , exchanges a gluon with the anti-quark, and then emits a gluon of momentum k_2 . Only one diagram of the eight that occur is shown.

We now consider the Feynman graphs, starting with Fig. 9. Once again we compute the imaginary part of the graph and consider the intermediate state as being on the energy shell. The propagator for the line (a) has the factor

$$(k_1 + z' p_\pi)^2 - m_q^2 = z' x_1 \nu + \dots, \quad (33)$$

while that of the near-mass-shell line (b) is independent of x_1 , because the quark momenta in the final state and in the pion wave function are not connected with the target momentum. The propagator of line (c) has the factor

$$(k_2 + q_1)^2 - m_q^2 = x_2 z \nu + \dots = x_1 z \nu + \dots. \quad (34)$$

Here q_1 is the momentum of the jet (z, κ_t) and \dots denotes the terms which are independent of x_1 . The last equation is obtained from using Eqs. (6,8). The results (33-34) show that the diagram of Fig. 9 takes on the mathematical form of the integral (32). Thus this term vanishes.

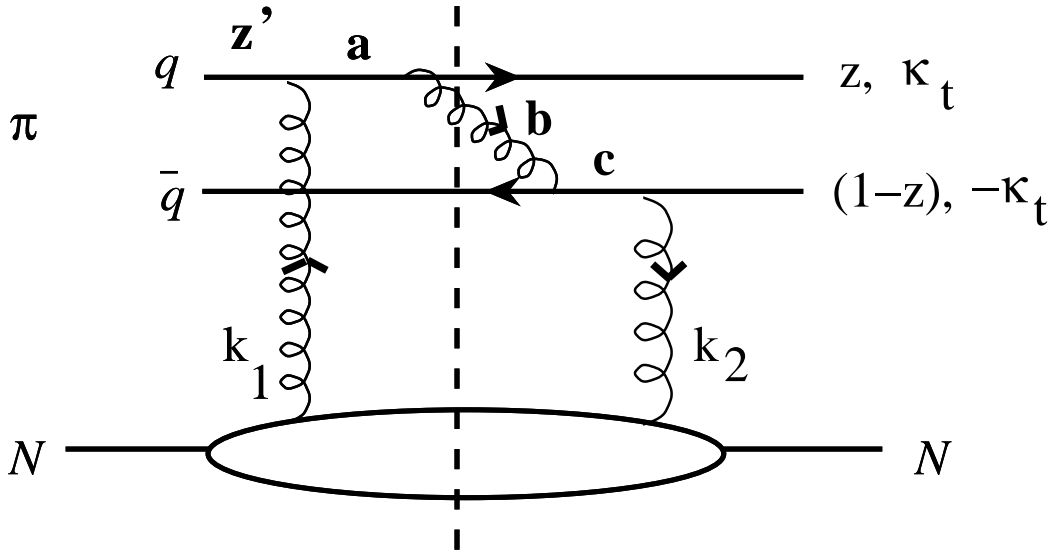


FIG. 10. Another contribution to $T_4 - T_{4d}$. The quark absorbs a gluon of momentum k_1 , exchanges a gluon with the anti-quark, and the anti-quark emits a gluon of momentum k_2 . Only one diagram of the four that contribute is shown.

We also consider the diagram of Fig. 10. In this case there are three propagators (a), (b), (c) that have a term proportional to $x_1\nu$, but the coefficients are not all positive. The propagator factor for line (a) is given by

$$(x_1 p_\pi + k_1)^2 = x_1 z' \nu + \dots, \quad (35)$$

while that of line (c) is given by

$$(k_2 + q_2)^2 - m_q^2 = x_2(1-z)\nu + \dots = (1-z)x_1\nu + \dots \quad (36)$$

At the same time, the coefficient multiplying x_1 in the propagator (b) (gluon production) has no definite sign. Thus for this diagram the integral over x_1 does not vanish. The presence of an additional gluon in the intermediate state means that $x_1 \propto x_2$. This and the use of the Weizsacker-Williams representation allow us to conclude that this diagram is suppressed by a power of κ_t^2 as compared to T_1 . Similar logic can be applied to any of the diagrams contributing to T_4 . The physical idea that the intermediate $q\bar{q}$ state does not live long enough to exchange a gluon is realized in the ability to close the contour of integration in the upper half plane or in the suppression by the power of κ_t^2 . The analyticity of the scattering amplitude in the upper half is a consequence of causality. Thus the physical and mathematical ideas behind the vanishing of T_4 are basically equivalent for all diagrams at high enough beam energies.

We conclude this section with a brief summary. We analyzed the leading diagrams for the pion dissociation into two jets and found that the hard dynamics-amplitude T_1 determines this process, with the initial state wave function determined by the hard gluon exchange diagram. In the next section we shall show that amplitudes T_2, T_3 are strongly suppressed by the requirement of the lack of radiation in the final state. This is because in the lowest order in α_s these amplitudes correspond to the propagation of a nonperturbative $q\bar{q}$ dipole or a $q\bar{q}g$ tripole over large longitudinal distances.

While we were revising the manuscript in response to referee's questions, a paper [38] appeared which claimed that, if one includes terms beyond the leading-logarithm approximation in $\alpha_s \ln x$, factorization does not hold and end-point singularities break collinear factorization. Our calculation shows that such problems are not present in the leading order approximation which keeps terms leading order in $\alpha_s \ln \frac{k_t^2}{\Lambda_{QCD}^2}$. The use of our light cone gauge, where the asymptotics of the fermion propagator has no infrared singularities in the hard regime, makes the separation of scales-QCD factorization- rather straightforward. Moreover in this gauge, terms $\sim \ln 1/x$ in the hard regime are related to the exchange by the gluon in the multi-Regge kinematics only [6]. As a consequence of the QCD factorization theorem terms $\sim \ln 1/x$ are included in structure functions of the target. On the contrary, if one uses the standard gauge $A^+ = 0$ or Feynman gauge, the cancellation of infrared singularities occurs if one includes the renormalization factor arising from the hard Fermion propagator, cf. discussion in Ref. [46]. Taking these terms together, the resulting amplitude contains no end-point singularity, and the factorization holds.

III. POST-SELECTION OF THE PROJECTILE WAVE FUNCTION BY FIXING THE FINAL STATE

A specific feature of the processes considered here is that the restriction on the composition of the final state selects a rather specific initial configuration of the projectile hadron. Following S.Nussinov (to be published) we denote such measurements as post-selection. In our case, the initial and final state wave functions are built at large longitudinal distances $\propto 1/2m_N x$, so there is plenty of time for radiation to occur. But our definition of the final state forbids radiation collinear to the direction of pion momentum. In particular, the relation between the transverse momentum of jet κ_t and the mass of the diffractively produced system, $M^2(2jet) = \kappa_t^2/z(1-z)$, is natural only for a $q\bar{q}$ final state. Thus any contribution due to processes for which such radiation is kinematically and dynamically permitted must be suppressed by the powers of Sudakov-type form factors and by a w_2 form factor. The first step is to analyze how the trigger for the two jet state restricts the composition of the final state.

A. Three jet production.

A question arises¹ whether the trigger used in Ref. [14] allows the separation of production by a $q\bar{q}$ state from the production by a $q\bar{q}g$ state (and more complicated states containing relatively soft partons) as the source of the observed dijets, and whether the presence of such states may change the κ_t dependence of cross section. Such states are certainly important in inclusive diffraction in DIS at HERA. A typical diagram corresponding to such a process is presented in Figure 11.

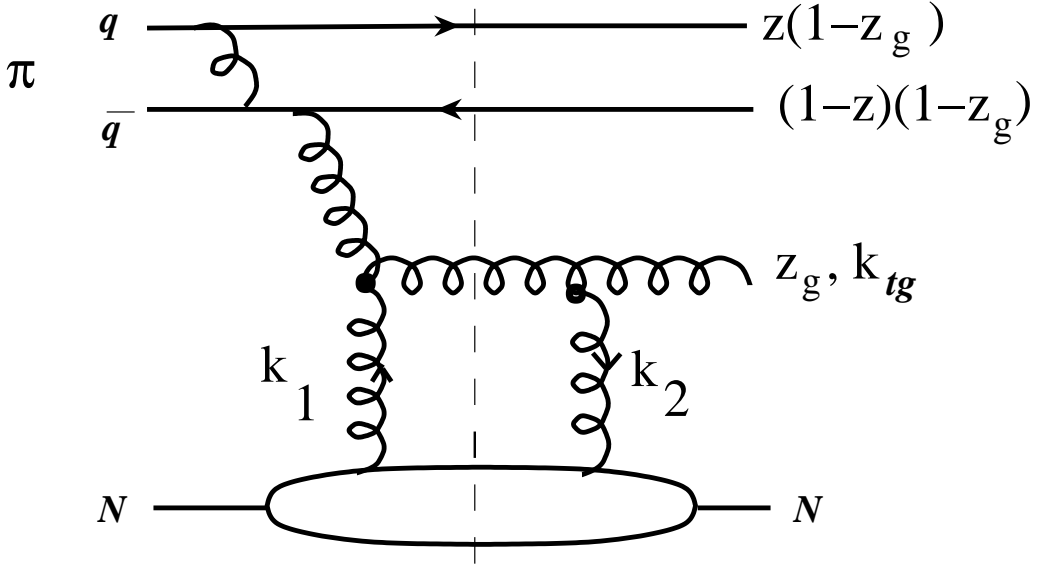


FIG. 11. A typical diagram corresponding to production of large mass $q\bar{q}g$ state.

An analysis of kinematics shows that the virtuality of the gluon interacting with the target is $\approx -\frac{(1-z_g)M_{2jet}^2+k_{tg}^2}{z_g}$ where z_g is the fraction of the pion momentum carried by a gluon in the final state and k_{tg} is its transverse momentum, and as usual, the mass of the final dijet system is given by $m_f^2 = M_{2jet}^2 = \kappa_t^2/z(1-z)$. The mass of a $q\bar{q}g$ system in the final state is given by $M_{3jet}^2 = \frac{M_{2jet}^2+k_{tg}^2}{(1-z_g)} + k_{tg}^2/z_g$. If $z_g \leq k_{tg}^2/M_{2jet}^2$ then $M_{3jet}^2 \geq 2M_{2jet}^2$, and therefore the $q\bar{q}g$ state is distinguishable from the two-jet state by the relation between κ_t^2 and the total mass. In this kinematics, the cross section depends on κ_t as $\alpha_s(k_{tg}^2)^3 \frac{(\alpha_s(k_{tg}^2)x_1 G(x_1, x_2, k_t^2))^2}{k_t^8}$. Beyond this kinematics, the cross section is additionally

¹ We thank J.Bjorken, and D.Soper for asking this question.

suppressed by the factor $\propto (z_g M_{2jet}^2)^{-2}$. Thus a contribution of such configurations is either dynamically suppressed, or distinguishable from the contribution of a $q\bar{q}$ configuration. Note also that the feature that k_{tg} is small would not lead to the cancellations needed for color transparency phenomenon to occur, and therefore the A-dependence would differ from what is observed.

It is important to be able to distinguish dijet production from the soft diffraction into a hadronic state having a total mass M_{diff}^2 and containing leading twist dijet production with mass M_{2jet}^2 . Evidently $M_{2jet}^2 \leq M_{diff}^2$. Cross section of such diffractive processes are often described as the hard diffractive mechanism of Ingelman-Schlein [39]. In this mechanism one considers a hard scattering of a parton belonging to the projectile π with a light-cone fraction x_π off a parton belonging to a diffractive parton density (effective Pomeron) with a light-cone fraction βx_P .

Here $1 - x_P$ is the nucleon momentum in the final state, cf [39]. It follows from the above definitions and energy-momentum conservation law that $R^{-1} \equiv \frac{M_{2jet}^2}{M_{diff}^2} = x_\pi \beta$. Thus R^{-1} is the fraction of the total mass of the diffractive state carried by two jets. We are interested in the paper in the limit when the mass of a diffractively produced hadronic state is carried mostly by 2 jets i.e. when $R \equiv R_0 \sim 1$. In this case the cross section for the production of dijets with $R \geq R_0$ (where R_0 being close to 1 is determined by the accuracy of measuring a fraction of the pion momentum carried by two jets) is

$$\frac{d\sigma}{d\kappa^2} \propto \frac{1}{M_{diff}^2} \kappa^{-4} \int_{R_0}^1 dx_\pi \int_{R_0/x_\pi}^1 d\beta (1 - x_\pi)^2 f_P(\beta). \quad (37)$$

Here a factor κ^{-4} is the usual κ dependence of the cross section of the hard two parton collision, $\frac{1}{M_{diff}^2}$ is the usual Pomeron flux factor, the factor $(1 - x_\pi)^2$ is the parametrization of the parton density in the pion at $x_\pi \rightarrow 1$, $f_P(\beta)$ is the diffractive structure function. Taking $f_P(\beta) \propto (1 - \beta)$ for $\beta \rightarrow 1$ (see e.g. [40]) we obtain $d\sigma/d\kappa^2(R \geq R_0) \propto (1 - R_0)^5/\kappa^6$. The factor $(1 - R_0)^3$ arises from the integration over x_π and factor $(1 - R_0)^2$ is from the integration over β . The additional factor $\frac{1}{\kappa_t^2}$ is because in the discussed region $M_{diff}^2 \approx M_{2jet}^2$. There is also a contribution of the Coherent Pomeron [41] corresponding to $\beta = 1$. It leads to a similar suppression as a function of R_0 : $\propto (1 - R_0)^4$.

Hence we conclude that the importance of the discussed leading twist mechanism as compared to the exclusive dijet production term which is $\propto \kappa^{-8}$ depends on the degree of exclusiveness of the experiment. The experiment [14] imposes the condition that $M_{2jet}^2 = M_{diff}^2$. Such a selection should have been rather efficient since due to the acceptance of the detector a condition was imposed that all produced pions should have momenta larger than a minimal one.

B. Suppression of the final state interaction

Let us consider the important consequences of the formulated above restrictions on the composition of the final state. The existence of the term T_3 displayed in Fig. 5, caused Jennings & Miller [42] to worry that the value of \mathcal{M}_N might be severely reduced due to a nearly complete cancellation. However, we shall explain here that this term as well as the term T_2 are strongly suppressed in QCD as compared to the naive PQCD calculation explained in Sect.II. This suppression is the only way to resolve an evident contradiction: the kinematic restriction on the final state discussed above forbids radiation collinear to the pion momentum, but such radiation naturally arises in a hard collision, or from the presence of a significant gluon admixture in the non-perturbative pion wave function when nonperturbative $q\bar{q}$ and more complicated configurations propagate large and increasing with energy longitudinal distances. It is convenient to represent this suppression as a product of two factors: $w = w_1 w_2$. The first factor accounts for the well understood suppression of the collinear initial state radiation in the scattering of a target gluon off a low k_t quark. Remember that by definition a non-perturbative pion wave function does not include a PQCD high momentum tail. Accounting for the LO QCD evolution will not change this conclusion in the LO approximation over parameter $\alpha_s \ln \frac{k_t^2}{\Lambda_{QCD}^2}$. In the case of the amplitude T_3 the diagrams where the hard gluon exchange is present both in the initial and the final states are potentially dangerous. However, this contribution into T_3 is suppressed by the power of α_s as compared to the amplitude T_1 . Similar radiation is permitted for the processes described by the amplitude T_3 because tripole $q\bar{q}g$ propagates large longitudinal distances. This radiation in the direction of pion momentum carries a finite fraction of pion momentum which is significantly larger than that for wee hadrons which are products of the jet fragmentation. These wee hadrons carry $\propto \frac{f_{ew} m_\pi}{M(2jet)}$ fraction of pion momentum. The w_1 form factor suppression for the amplitude T_3 is given by the square of Sudakov type form factor: $S^2(\kappa_t^2/l_t^2)$; one form factor arises for each collision with a target gluon. Here l_t is the transverse momentum of a quark within the non-perturbative pion wave function. This form factor is a square root of the form factor of quark [43] because the radiation of gluons off the final quark is included in the definition of the final state. In the light cone gauge:

$$w_1 = S^2(\kappa_t^2/l_t^2) = \exp(-4/3 \frac{\alpha_s}{4\pi} \ln^2 \kappa_t^2/l_t^2), \quad (38)$$

where, using the leading log approximation, we replaced k_{1t} by κ_t in the argument of the Sudakov form factor. Recall that the form factor S^2 is exactly the Sudakov form factor which enters in the Dokshitzer-Gribov-Lipatov-Altareli-Parisi evolution equations as a coefficient of the $\delta(x-1)$ term, see the discussion in Ref. [44].

w_1 form factor should be practically the same for both amplitudes T_2 and T_3 . This is because of total transverse momentum of the system of high k_t quark(antiquark) + high k_t gluon in the amplitude T_3 is small and controlled by the nonperturbative pion wave function. Therefore in the collision with a target gluon this quark(antiquark) - gluon system radiates in the direction of pion momentum as a single quark(antiquark).

The second suppression factor, w_2 , accounts for the dependence of the form of the effective QCD Lagrangian and appropriate degrees of freedom on the resolution. As a result of partial conservation of axial current f_π is independent on the resolution-invariant on renormalization group transformations. At the same time important degrees of freedom depend on the resolution: dominant degrees of freedom in hard processes are bare quarks. On the contrary, in the non-perturbative regime because of the effects of spontaneously broken chiral symmetry dominant degrees of freedom are constituent quarks, pseudogoldstone modes -pions, various condensates of quark, gluon fields, etc. Remember that for the average-sized configuration of a hadron, approximately half of the pion momenta is carried by gluons. (Within a constituent quark model renormalizability of QCD is usually accounted for by introducing effective mass and effective interaction for the constituent quarks and f_π is calculated in these models in terms of the constituent but not bare quarks. The evaluation of f_π within a bag model should include a prescription how to treat the nonperturbative volume energy density - bag surface. Within the Weizecker-Williams approximation this energy is equivalent to the gluon cloud in the light cone wave function of a pion .)

In the case of interaction of local current f_π is calculable in terms of the distribution of bare quarks which accounts for both nonperturbative and perturbative effects [46]. In this case the suppression factor w_2 tends to one for $k_0^2 \rightarrow \infty$ since in this case only short distance perturbative degrees of freedom survive. So amplitude T_1 contains no additional suppression factor w_2 . On the contrary in the amplitudes T_2, T_3 the structure of constituents in the non-perturbative pion distribution is resolved as a result of a large time interval between two consequent hard collisions of pion constituents off target gluons. A hard collision of the pion's constituents with target gluons (with momentum transfer ($k_0^2 \ll \kappa^2$)) frees some gluons from the pion wave function, and emitted radiation is collinear to the pion momentum. This radiation is, however, forbidden by the restriction on the final states discussed above. Thus the selection of a component of the pion wave function of a size determined by non-perturbative QCD, leads to an additional factor w_2 which suppresses this contribution to the scattering amplitude.

We may estimate the factor w_2 using models as follows:

$$w_2 = \frac{\int_0^1 dz_1 \int_0^1 dz_2 (1-z_1-z_2)^n \theta(\delta-1+z_1+z_2) \theta(1-z_1-z_2)}{\int_{0,1} dz_1 dz_2 (1-z_1-z_2)^n \theta(1-z_1-z_2)} = (n+2)(\delta)^{n+1}. \quad (39)$$

Here $z_{1,2}$ are the fractions of the pion momentum carried by jets in the final state, and δ is the experimental uncertainty in the fraction of pion momentum carried by high κ_t dijets. Within the democratic chain approximation, which reasonably describes the Q^2 and x dependencies of hard exclusive processes, the value of $n = 1$ for the component which contains $q\bar{q}$ and a valence gluon. Another estimate of n can be obtained in the constituent quark model assuming, for simplicity, that each constituent quark consists of a bare quark and one gluon. In this case we are effectively dealing with a four particle system and hence $n \geq 2$. The factor w_2 gives a significant numerical suppression for all the models. No such suppression appears in the amplitude T_1 because the radiation of a gluon with small transverse momentum from a highly localized (e.g. size $1/\kappa_t$) color-neutral quark configuration is suppressed by a power of κ_t^2 . (Note that in the case of the final state interaction, the non-perturbative pion wave enters at 0 inter-quark transverse distances. This means that gluon radiation with transverse momenta, $k_{tg}^2 \leq l_t^2$, should be suppressed. For gluon radiation with larger transverse momenta there is no restriction.) Amplitudes T_2, T_3 correspond to the propagation at large longitudinal distances of "large" size $q\bar{q}$ pair whose transverse size is controlled by non-perturbative pion wave function. The net result of all of this is that amplitudes T_2, T_3 and Figs. 3,5,6 can be neglected and we shall therefore ignore the amplitudes T_2, T_3 .

We also observe that the contribution of Feynman diagrams in which the skewed distribution is modeled by the scattering of an on-shell quark or gluon is suppressed even further by the square of the Sudakov form factor, in addition to form factors w_1, w_2 .

C. Non-leading order approximation to the dipole-target interaction

In the previous section we used the leading $\alpha_s \ln \kappa_t^2 / \Lambda_{QCD}^2$ approximation (for the case $k_{1,2t}^2 \ll \kappa_t^2$) to estimate diagrams. To go beyond this, one should take into account the contribution of the region $k_{i,t}^2 \approx \kappa_t^2$ to obtain the $q\bar{q}$ dipole-target interaction. The related contribution to dijet production is denoted as T_5 . To some extent this contribution has been discussed above, in relation to the amplitude T_4 . For the amplitude T_5 , quarks in the wave function of the initial pion have small transverse momenta l_t , and there is no hard interaction between the q and \bar{q} in the initial or final states, see Fig. 12.

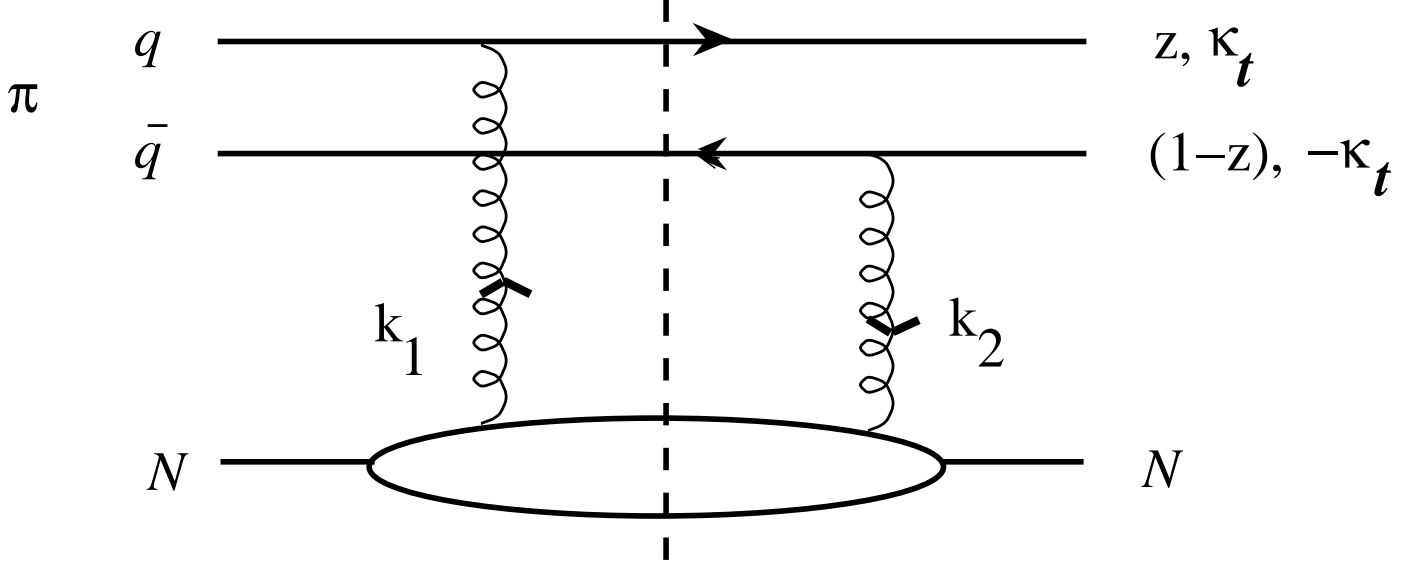


FIG. 12. T_5 , Hard color flow diagram.

Let us outline various phenomena relevant for the smallness of this contribution as compared to T_1 .

1. The amplitudes given by diagram Fig. 12 correspond to two hard collisions occurring at the different space-time points where color abruptly changes the direction of its motion. The longitudinal distances (time interval) between both hard collisions are large, $\approx 2E_\pi/\kappa_t^2$, so that the emission of gluon radiation is permitted. The difference in impact parameters characterizing both hard collisions is $\approx \frac{\pi}{2l_t}$, where l_t is the transverse momentum of quark in the non-perturbative pion wave function. Thus collinear gluon radiation in both collisions is not canceled, and forward gluon bremsstrahlung (precluded in T_1 by the localization of color in transverse space) occurs. Such radiation effects are precluded by our choice of final states for which radiation collinear to pion momentum is absent. Thus the ratio T_5/T_1 is suppressed (as explained in the previous subsection) by the square of a Sudakov-type form factor: $S^2(\kappa_t^2/l_t^2) = \exp(-4/3 \frac{\alpha_s}{4\pi} \ln^2 k_{1t}^2/l_t^2)$. Including the effects of the Sudakov type form factor leads to an increase of the effective value l_t with an increase of k_{1t} , and therefore will change kinematics of this diagram in the direction to that for the term T_1 .
2. Final states with additional gluons collinear to pion momentum are initiated by the components of the pion wave function which are close to the average. The significant probability for such processes follows from the fact that the gluons carry $\sim 1/2$ of the pion momentum. Thus the selection of the component of a pion wave function of average size, but having no gluons, leads again to the appearance of the additional suppression factor w_2 .
3. As the consequence of the rapid decrease of the non-perturbative pion wave function with l_t^2 for the diagrams of Fig. 12, the target gluon actually has a negative value of x_2 . To see this, we apply Eq. (30) to the situation when the transverse momenta of quarks in the initial state l_t are much smaller than κ_t , so that $k_{1t} \sim \kappa_t, k_{2t} \sim -\kappa_t$. In this case

$$x_2 = \frac{1}{\nu} \left[\frac{\kappa_t^2}{1 - \beta - z} - \frac{\kappa_t^2}{z(1 - z)} \right]. \quad (40)$$

Here β is the fraction of the pion momentum carried by a target gluon. To satisfy the condition $x_2 > 0$ one needs

$$1 - z > \beta > (1 - z)^2, \text{ or } z > \beta > z^2. \quad (41)$$

This condition cannot be satisfied within the leading $\log 1/x$ approximation where $\beta \ll 1$. Moreover, Eq. (40) implies that $-x_2\nu \propto \kappa_t^2$, except for a narrow interval in β near $\beta = (1 - z)^2$. The contribution of this narrow interval is suppressed by the small length of this interval. (The end point $z \sim 0, z \sim 1$ contributions are suppressed by the pion wave function.) In the non-perturbative regime- within the parton model- the contribution of the $x_2 \leq 0$ region cannot be expressed in terms of the unintegrated gluon density, and it is suppressed by power of $1/\kappa_t^2$ [7]. On the contrary, within the leading $\log 1/x$ approximation such a strong suppression is substituted by a slower one whose value depends on the ratio of κ_t^2 to the square of the mass of the recoil system (the wave function of a target where a high κ_t gluon is removed). This ratio is $\kappa_t^2/\beta\nu$. Evidently, the contribution of small β is suppressed by the rapid decrease of structure function with κ_t^2 . This cutoff is significantly stronger than that for the term T_1 because of smaller transverse momenta of target gluons.

Thus we conclude that the selection of the final state leading to the post-selection of the initial state shows that approximation of having a point-like pionic configuration in the final state should be valid even beyond the leading order approximation used in this paper. Therefore formulas representing a hard process as the convolution of a pion wave function with the interaction cross section [5] should be valid beyond the LO approximation.

It has been suggested in [45] that gluon scattering off on-mass shell quarks and gluons in the target wave function, see Fig. 12, is the dominant process for the diffractive dijet production by a nuclear target. We explained above that in QCD this amplitude is suppressed as compared to the term T_1 by the product of the square of Sudakov type form factors and the form factor w_2 . So we will neglect now and forever the amplitudes presented in Fig. 12 .

IV. AMPLITUDE FOR $\pi N \rightarrow NJJ$ —EVALUATION OF THE DOMINANT TERM

Let us consider the forward ($t = t_{min} \approx 0$) amplitude, \mathcal{M} , for coherent dijet production on a nucleon $\pi N \rightarrow NJJ$ [5]:

$$\mathcal{M}(N) = \langle f(\kappa_t, z), N' | \hat{f} | \pi, N \rangle, \quad (42)$$

where \hat{f} represents the interaction with the target nucleon. The initial $|\pi\rangle$ and final $|f(\kappa_t, z)\rangle$ states represent the physical states which generally involve all manner of multi-quark and gluon components. For large enough values of κ_t , the result of calculations can be represented in a form in which only the $q\bar{q}$ components of the initial pion are relevant in Eq. (42). This is because we are considering a coherent nuclear process which leads to a final state consisting of a quark and anti-quark moving at high relative transverse momentum.

We showed above that the dominant (in powers of s and κ_t^2) Feynman diagrams will be expressed in terms of the light-cone wave function of the pion. We therefore begin by calculating the high transverse momentum component of the pion wave function. The non-perturbative component of the light-cone pion wave function is represented by $|\pi\rangle$, and the high momentum components can be treated as arising from the following approximate equation [46]:

$$|\pi_{q\bar{q}}\rangle = G_0 V_{eff} |\pi\rangle, \quad (43)$$

where $G_0(p_t, y)$ is the non-interacting $q\bar{q}$ Green's function for $p_t^2 \gg m_q^2, m_\pi^2$

$$\langle p_t, y | G_0 | p'_t, y' \rangle = \frac{\delta^{(2)}(p_t - p'_t) \delta(y - y')}{-\frac{p_t^2}{y(1-y)}}, \quad (44)$$

in which m_q represents the quark mass, y and y' represent the fraction of the longitudinal momentum carried by the quark; and the relative transverse momentum between the quark and anti-quark is p_t . The complete effective interaction, obtainable in principle from PQCD, implicitly includes the effects of all Fock-space configurations.

The evaluation of the graphs corresponding to Fig. 1 consists of two parts. As a first step, the Feynman diagram of Fig. 1 can be rewritten as a product of a high momentum component of a light cone pion wave function with the amplitude for the scattering of a quark-anti-quark dipole by a target. So, we need to know the relevant part of the pion wave function. Secondly, we need to determine the interaction with the target (here with the gluon field of the target) which causes the pion to dissociate into a $q\bar{q}$.

A. High momentum component of the light cone pion wave function²

The full wave function $|\pi\rangle$ is dominated by components in which the separation between the constituents is of the order of the diameter of the physical pion. But there is a perturbative tail in momentum space which accounts for the short distance part of the pion wave function. This tail is of dominant importance here because we take the overlap with a final state constructed from constituents moving at high relative momentum. It is therefore reasonable to start our considerations from the one gluon exchange contribution V^g , and use the light cone gauge: $p'_\pi{}^\mu A^\mu = 0$ and the Brodsky-Lepage [46] normalization and phase-space conventions. Here $p'_\pi = p_\pi - c \cdot p_N$ where c is determined from the condition: $p'_\pi{}^2 = 0$. Evidently for sufficiently high energies of pion projectile such a gauge will almost coincide with the gauge $A_- = 0$ and therefore the Wilson line operator between $q\bar{q}$ pair: $\exp(i \int A_\mu dx_\mu) \approx \exp(i \int A_t dx_t)$. Thus in the target rest frame, at the light cone where $x_- = 0$ the Wilson line operator does not produce additional gluons in spite of the large and increasing with energy longitudinal distances x_+ . The wave function $\chi(k_t, x)$ is gauge invariant because it depends on transverse, i.e. on physical degrees of freedom. (On the contrary in the Feynman gauge the $q\bar{q}$ pair evolves into a many particle state because of the Wilson line operator. So a calculation in the Feynman gauge should include the evaluation of the form factor which guarantees dominance of the two particle final state.) Another advantage of the gauge chosen in the paper is that the amplitude for hard gluon exchange has no infrared divergences and therefore the separation between large and small distances is straightforward. (On the contrary in the gauge $A^+ = 0$ the amplitude for hard gluon exchange is infrared divergent. The divergent contribution is, however, exactly canceled out with that in the fermion propagator in this gauge, cf. [46].) The chosen gauge is convenient to evaluate the high momentum component of the pion wave function. For the evaluation of the parton distribution within a nucleon another gauge is more appropriate. This mismatch does not introduce, however, additional problems because the factorization theorem justifies the possibility to choose independently the gauges for the amplitude of pion fragmentation into jets and for the parton distribution within a nucleon. The perturbative tail is obtained as the result of the one gluon exchange interaction acting on the soft part of the momentum space wave function, defined as

$$\psi(l_t, y) \equiv \langle l_t, y | \pi \rangle_{q\bar{q}}. \quad (45)$$

By definition, ψ is dominated by its non-perturbative low-momentum components. However, the amplitude we compute depends on the high momentum tail, χ . For this component, perturbation theory is applicable and we use the one-gluon exchange approximation to the exact $q\bar{q}$ wave function of Eq. (45) to obtain χ , valid for large values of κ_t , as

$$\chi(k_t, x) = -4\pi C_F \frac{1}{\left[m_\pi^2 - \frac{k_t^2 + m_q^2}{x(1-x)} \right]} \int_0^1 dy \int \frac{d^2 l_t}{2(2\pi)^3} V^g(k_t, x; l_t, y) \psi(l_t, y) \quad (46)$$

with

$$V^g(k_t, x; l_t, y) = \alpha_s \frac{\bar{u}(x, k_t)}{\sqrt{x}} \gamma_\mu \frac{u(y, l_t)}{\sqrt{y}} \frac{\bar{v}(1-x, -k_t)}{\sqrt{1-x}} \gamma_\nu \frac{v(1-y, -l_t)}{\sqrt{1-y}} d^{\mu\nu} \\ \times \left[\frac{\theta(y-x)}{y-x} \frac{1}{m_\pi^2 - \frac{k_t^2 + m_q^2}{x} - \frac{l_t^2 + m_q^2}{1-y} - \frac{(k_t - l_t)^2}{y-x}} + (x \rightarrow 1-x, y \rightarrow 1-y) \right], \quad (47)$$

where $C_F = \frac{n_c^2 - 1}{2n_c} = \frac{4}{3}$, and $d^{\mu\nu}$ is the projection operator of the gluon propagator evaluated in the light cone gauge defined above: $d_{\mu,\nu} = \delta_{\mu,\nu} - \frac{p'_\mu(\pi)k_\nu + k_\mu p'_\nu(\pi)}{(p'_\pi k)}$. Here k is the gluon four-momentum. The range of integration over l_t is restricted by the non-perturbative pion wave function ψ .

Then in the evaluation of V^g we set m_q and l_t to 0 everywhere in the spinors and energy denominators. This is legitimate because of a lack of infrared divergences in the amplitude of hard process [17].

Thus

$$V^g(k_t, x; l_t, y) \approx \frac{\alpha_s(k_t^2)}{x(1-x)y(1-y)} V(x, y) \quad (48)$$

²An early version of this subsection which did not include discussion of renormalization effects has appeared in [17].

where in the lowest order over coupling constant α_s but keeping leading power of k_t^2 :

$$V(x, y) = 2 [(\theta(y-x)x(1-y) + \theta(y-x)) + (x \rightarrow 1-x, y \rightarrow 1-y)], \quad (49)$$

We want to draw attention that in the gauge chosen in the paper dominant contribution arises from the components of gluon propagator transverse to the directions of pion and nucleon four momenta.

The net result for the high k_t component of the pion wave function is then

$$\chi(k_t, x) = \frac{4\pi \ 2 \ C_F \alpha_s(k_t^2)}{k_t^2} \int_0^1 dy V(x, y) \frac{\phi(y, k_t^2)}{y(1-y)}, \quad (50)$$

where nonperturbative support

$$\phi(y, k_t^2) \equiv \int \frac{d^2 l_t}{2(2\pi)^3} \theta(k_t^2 - l_t^2) \psi(l_t, y). \quad (51)$$

The analysis of experimental data for virtual Compton scattering and the pion form factor performed in [48,49] shows that this amplitude is not far from the asymptotic one [47] for $k_t^2 \geq 2 - 3 \text{ GeV}^2$,

$$\phi(k_t^2 \rightarrow \infty, y) = a_0 y(1-y), \quad (52)$$

where $a_0 = \sqrt{3} f_\pi$ with $f_\pi \approx 93 \text{ MeV}$.

Equation (50) represents the high relative momentum part of the pion wave function in the lowest order of pQCD when running of the coupling constant is neglected. Using the asymptotic function (52) in Eq. (50) leads to an expression for $\chi(k_t, x) \propto x(1-x)/k_t^2$

$$\chi(k_t, x) = \frac{4\pi C_F \alpha_s(k_t^2)}{k_t^2} a_0 x(1-x). \quad (53)$$

The next step is to use the renormalization invariance of theory to include the k_t dependence of the coupling constant :

$$\alpha_s(k_t^2) = \frac{4\pi}{\beta \ln \frac{k_t^2}{\Lambda^2}}, \quad (54)$$

with $\beta = 11 - \frac{2}{3} n_f$. This can be easily done similar to [46] where the relationship between $\phi(Q^2, x)$ and $\chi(k_t, x)$ and QCD evolution equation for $\phi(Q^2, x)$ have been deduced.

The quark distribution function $\phi(x, Q^2)$ -the amplitude for finding constituents with longitudinal momentum x in the pion which are collinear up to the scale Q^2 is [46]

$$\phi(x, Q^2) = \frac{1}{d_f(\kappa_t^2)} \int_0^{Q^2} \chi(k_t^2, x) \frac{dk_t^2}{16\pi^2}. \quad (55)$$

The factor : $\frac{1}{d_f(\kappa_t^2)} = (\ln \frac{Q^2}{\Lambda_{QCD}^2})^{-\gamma_F/\beta}$ arises from vertex and self-energy corrections. (By definition the running coupling constant includes the renormalization factor of the fermion propagator. Such a renormalization factor is absent in the definition of $\chi(k_t, x)$). One of advantages of the gauge chosen in this paper is that γ_F

$$\gamma_F = C_F, \quad (56)$$

has no infrared divergences in difference from [46] where gauge A_+ has been chosen. Calculations are significantly simplified because the dominant contribution is given by transverse gluon polarizations only. The evolution equation for $\phi(x, Q^2)$ gives [46,47]

$$\phi(x, Q) = x(1-x) \sum_{n=0}^{\infty} a_n C_n(1-2x) \left(\frac{\ln Q^2}{\Lambda_{QCD}^2} \right)^{-\gamma_n}, \quad (57)$$

where $\gamma_n = \frac{C_F}{\beta} (1 - \frac{2}{(n+1)(n+2)} + 4 \sum_{k=2}^{k=n+1} 1/k)$, $C_n(1-2x)$ are Gegenbauer polynomials. Coefficients a_n are the subject of discussions in the literature and they can be estimated within the current models. The above equation makes it possible to calculate the high k_t behavior of $\chi(k_t, x)$ as

$$\frac{\chi(k_t^2 = Q^2, x)}{16\pi^2} = \frac{d \left[\phi(x, Q) \left(\ln \frac{Q^2}{\Lambda_{QCD}^2} \right)^{\gamma_F/\beta} \right]}{dQ^2}. \quad (58)$$

Thus the z, κ_t dependence of the cross section for the diffractive dijet production should be sensitive at moderately large k_t to the terms involving Gegenbauer polynomials of the order greater than 0 in the pion wave function if a_n are sufficiently large. The process of the photoproduction of jets at HERA will be appropriate for this purpose.

It follows from the above equation that the asymptotic wave function is as follows:

$$\chi(k_t, x) = \frac{4\pi C_F \alpha_s(k_t^2)}{k_t^2} a_0 x(1-x) \left(\ln \frac{Q^2}{\Lambda_{QCD}^2} \right)^{C_F/\beta}. \quad (59)$$

Thus QCD predicts the dependence of $\chi(k_t, x)$ to be of the form used in Ref. [5].

B. Interaction with the target

To compute the amplitude T_1 it is necessary to specify the scattering operator \hat{f} . We will fix the transverse recoil momentum of the target at zero to simplify the discussion. The transverse distance operator $\vec{b} = (\vec{b}_q - \vec{b}_{\bar{q}})$ is canonically conjugate to $\vec{\kappa}_t$. At sufficiently small values of b , the leading twist effect and the dominant term at large s arises from diagrams in which the pion fragments into two jets as a result of interactions with the two-gluon component of the gluon field of a target, see Fig. 1. The perturbative QCD determination of this interaction, which is a type of QCD factorization theorem, involves a diagram similar to the gluon fusion contribution to the nucleon sea-quark content observed in deep inelastic scattering. One calculates the box diagram for large values of κ_t using the wave function of the pion instead of the vertex for $\gamma^* \rightarrow q\bar{q}$. The application of the technology leading to the QCD factorization theorem in the impact parameter space leads [12,5,18,50] to

$$\hat{f}(b^2) = is \frac{\pi^2}{3} b^2 [x_N G_N(x_N, Q_{\text{eff}}^2) + 2/3 x_N S_N(x_N, Q_{\text{eff}}^2)] \alpha_s(Q_{\text{eff}}^2), \quad (60)$$

in which G_N is the gluon distribution function of the nucleon, S_N is the sea quark distribution function of the nucleus for a flavor coinciding with that of the $q\bar{q}$ dipole, and $Q_{\text{eff}}^2 = \frac{\lambda}{b^2}$. The factor 2/3 appearing in the second term is the same as in the LO approximation for the longitudinal structure function and exclusive vector meson production [51]. The only difference is that in our case the number of flavors is unity. For our kinematics, it is reasonable to use $\lambda(x = 10^{-3}) = 9$ [25]. The formula (60) should be modified when applied to hard diffractive processes. The mass difference between the pion and the final two-jet state requires that the reaction proceeds by a non-zero momentum transfer to the target. This means that the function G_N should be replaced by the skewed (or off-diagonal or generalized) gluon distribution. Thus the distribution function should depend on the plus components x_1, x_2 of the momenta k_1, k_2 of the two exchanged gluons, Eq. (7).

The difference between the skewed and ordinary gluon distribution is calculable in QCD using the evolution equation for the skewed parton distributions [11,52]. The kinematical relation between x_1 and $x_1 - x_2$ is given in Eq. (6). But x_1 is close to x_N of Eq. (61), while x_2 is small in the calculation of T_1 . The skewed parton distribution can be approximated by a gluon distribution [53,54] if

$$x_N \approx (x_1 + x_2)/2 \approx \frac{\kappa_t^2}{2z(1-z)s}. \quad (61)$$

While including the effect of skewedness would alter any detailed numerical results, the qualitative features of the present analysis would not be changed.

The most important effect shown in Eq. (60) is the b^2 dependence, which shows the diminishing strength of the interaction for small values of b . To simplify formulas it is convenient to rewrite σ in the form:

$$\hat{f}(b^2) = is \frac{\sigma_0}{\langle b_0^2 \rangle} b^2 = is \frac{\sigma_0}{\langle b_0^2 \rangle} (-\nabla_{\kappa}^2), \quad (62)$$

in which the logarithmic dependence of α_s and the gluon distribution on b^2 are included in σ_0 . It is easy to check by direct calculations of Feynman diagrams that the operator ∇_{κ}^2 acts on the transverse momentum variables of the pion wave function. Our notation is that $\langle b_0^2 \rangle$ represents the pionic average of the square of the transverse separation, and within the leading log accuracy

$$\frac{\sigma_0}{\langle b_0^2 \rangle} \approx \frac{\pi^2}{3} \alpha_s(\kappa_t^2) [x_N G_N^{(skewed)}(x_1, x_2, \kappa_t^2)], \quad (63)$$

in which the ordinary gluon distribution is used as the initial condition for the QCD evolution equation for the skewed/generalized gluon density. This result is a factor of four smaller than presented in Ref. [5].

The result (63) holds for x_N about 10^{-2} . For x_N of about 10^{-3} or smaller, the second kinematic regime mentioned in the introduction is relevant, and one would obtain different results. For still smaller values of x , say $x \sim 10^{-5}$ non-linear gluonic effects become important, and the present treatment of the $q\bar{q}$ interaction with the target may be insufficient.

C. One Gluon Exchange in the Pion- T_1

The necessary inputs to evaluating T_1 are now available. The approximate pion wave function, valid for large relative momenta, is given by Eq. (53). The interaction \hat{f} is given by Eq. (62). The use of Eq. (62) allows a simple evaluation of the scattering amplitude T_1 because the b^2 operator acts on the pion wave function (here σ_0 is treated as a constant) as $-\nabla_{\kappa_t}^2$, leading to the result

$$T_1 = -4is \frac{\sigma_0}{\langle b^2 \rangle} \frac{4\pi C_F \alpha_s(\kappa_t^2)}{\kappa_t^4} \left(\ln \frac{k_t^2}{\Lambda_{QCD}^2} \right)^{\frac{C_F}{\beta}} a_0 z(1-z). \quad (64)$$

This amplitude T_1 is of the same form as our 1993 result [5]. The present result is obtained directly from QCD, in contrast with the earlier work which used some phenomenology for the pion wave function.

Corrections to Eq.(64) are of the order $\frac{1}{\ln \frac{\kappa_t^2}{\Lambda^2}}$. For example, a literal application of Eq. (62) would lead to a factor

$\left(1 + \frac{2}{\ln \frac{\kappa_t^2}{\Lambda^2}} \right)$. However, similar corrections may arise from other effects not considered here. So a calculation of such corrections is beyond the scope of this paper.

Our κ_t dependence of T_1 leads to: $\frac{d\sigma(\kappa_t)}{d\kappa_t^2} \propto \frac{\left(\ln \left(\frac{\kappa_t^2}{\Lambda_{QCD}^2} \right) \right)^{2C_F/\beta}}{\kappa_t^8}$ for $x_N \sim 10^{-2}$. This can be understood using simple reasoning. The probability of finding a pion at $b \leq \frac{1}{\kappa_t}$ is $\propto b^2$, while the square of the total cross section for small-dipole-nucleon interactions is $\propto b^4$. Hence the cross section of productions of jets with sufficiently large values

of κ_t integrated over d^2k_t is $\propto \frac{\alpha_s(\kappa_t^2)^2 \left(\ln \left(\frac{\kappa_t^2}{\Lambda_{QCD}^2} \right) \right)^{\frac{2C_F}{\beta}}}{\kappa_t^6}$, for $x_N \sim 10^{-2}$, leading to a differential cross section $\propto \frac{1}{\kappa_t^8}$. This reasoning ignores the dependence of the gluon structure function on κ_t . For sufficiently small values of $x(x \sim 10^{-3})$, gluon evolution would give a somewhat different behavior.

V. NUCLEAR DEPENDENCE OF THE AMPLITUDE

The picture we have obtained is that the amplitude is dominated by a process in which the pion becomes a $q\bar{q}$ pair of essentially zero transverse extent well before hitting the nuclear target. This point-like configuration (PLC) can move through the entire nucleus without expanding. The $q\bar{q}$ can interact with one nucleon and can pass undisturbed through any other nucleon. For zero momentum transfer q_t to the nucleus, the amplitude $\mathcal{M}(A)$ takes the form

$$\mathcal{M}(A) = A \mathcal{M}(N) \frac{G_A(x_1, x_2, m_f^2)}{AG_N(x_1, x_2, m_f^2)} \left(1 + \frac{\epsilon}{\langle b^2 \rangle > \kappa_t^2} A^{1/3} \right) \equiv A \mathcal{M}(N) \Gamma, \quad (65)$$

in which the skewedness of the gluonic distribution is made explicit, and where the real number $\epsilon > 0$. Observe the factor A which is the dominant effect here. This factor is contained in the ratio of gluon distributions in a nucleus and in a nucleon [5]. This dependence on the atomic number is a reliable prediction of QCD in the limit m_f^2 and $s \rightarrow \infty$, with fixed x_N (of Eq. (61)). (The quantity m_f is the mass of the dijet system.) On the contrary, for $x_N \rightarrow 0$ with fixed m_f^2 , the nuclear shadowing of the gluon distribution becomes very important [5,36].

The ϵ correction term in Eq. (65) is a higher twist contribution which arises from a single rescattering which can occur as the PLC moves through the nuclear length ($R_A \propto A^{1/3}$). That $\epsilon > 0$ was a somewhat surprising feature of our

1993 calculation because the usual second order rescattering, as treated in the Glauber theory, always reduces cross sections. This highly unusual sign follows from the feature in QCD that the relative contribution of the rescattering term (screening term) decreases with increasing size of the spatially small dipole. The key features of the usual first order term are $f = i\sigma$, and those of the usual second order term are $if^2 = -i\sigma^2$. Note the opposite signs. For us here $f = i\sigma_0 b^2 / \langle b^2 \rangle$, For very large values of κ_t^2 the operator b^2 , as applied to the pion wave function χ , which falls with κ_t^2 as $1/\kappa_t^2$ gives $b^2\chi = -\frac{4\chi}{\kappa_t^2}$. So the first term $f\chi = -i4\sigma_0/(\langle b^2 \rangle \kappa_t^2)\chi$ now has the same sign as the second-order term: $if^2\chi = -i[\sigma_0/\langle b^2 \rangle b^2]^2\chi = -i32[\sigma_0/(\langle b^2 \rangle \kappa_t)]^2\chi$

The differential cross section takes the form

$$\frac{d\sigma(A)}{dq_t^2} = A^2\Gamma^2 \frac{d\sigma(N)}{dt} e^{tR_A^2/3}, \quad (66)$$

for small values of t . Note that

$$-t = q_t^2 - t_{\min}, \quad (67)$$

where $-t_{\min}$ is the minimum value of the square of the longitudinal momentum transfer:

$$-t_{\min} = \left(\frac{m_f^2 - m_\pi^2}{2p_\pi} \right)^2. \quad (68)$$

Our discussion below is applicable in the kinematics where $-t_{\min}R_A^2/3 \leq 1$ so that the entire dependence of the cross section on t_{\min} is contained in the factor $e^{t_{\min}R_A^2/3}$.

One measures the integral

$$\sigma(A) = \int dt \frac{d\sigma(A)}{dt} = \frac{3}{R_A^2} A^2 \Gamma^2 \sigma(N). \quad (69)$$

A typical procedure is to parametrize $\sigma(A)$ as

$$\sigma(A) = \sigma_1 A^\alpha \quad (70)$$

in which σ_1 is a constant independent of A. For the R_A corresponding to the two targets Pt ($A = 195$) and C ($A = 12$) of E791, one finds $\alpha \approx 1.45$. The experiment [14] does not directly measure the coherent nuclear scattering cross section. This must be extracted from a measurement which includes the effects of nuclear excitation. The extraction is discussed below.

As pointed out previously [17], the values of our multiple scattering correction of our 1993 calculation [5] were overestimated by a factor of approximately four. This is because the σ_0 was chosen to be larger by a factor of 4 than in [18] and in Eq. (60). We now find that for values of κ_t greater than about 2 GeV, the coefficient α could be enhanced by between 0.0 and 0.08, depending on the value of κ_t . Taking 0.04 as a mean value one finds $\alpha \approx 1.5$. This estimate depends on the use of a model for the non-perturbative part of $|\pi\rangle$, and also on the validity of a simple eikonal treatment for the multiple-scattering corrections which is questionable at the high energies that we consider here.

Another potentially important A-dependent effect is the nuclear shadowing of the parton densities. Very little direct experimental information is available for the A-dependence of the gluon structure function. The analyses of the data combined with the momentum sum rules and the calculation of gluon shadowing at small x suggest that the value $x \sim 0.01$ (which corresponds to the kinematics of [14]) is in a transition region between the regime of an enhancement of the gluon distribution at $x \sim .1$ and the strong shadowing at $x \leq 0.005$ [20–23]. Using the A-dependence of F_{2A} as a guide, and in particular the NMC ratio F_{2Sn}/F_{2C} [24], the shadowing may reduce α for the [14] kinematics by $\Delta\alpha \sim -0.08$.

VI. EXPERIMENTAL CONSIDERATIONS

The requirements for observing the influence of color transparency were discussed in 1993 [5]. The two jets should have total transverse momentum to be very small. The relative transverse momentum should be greater than about ≥ 2 GeV and the mass of the diffractive state should be described by the formula

$$m_f^2 = \frac{m_q^2 + \kappa_t^2}{z(1-z)}. \quad (71)$$

Maintaining this condition is necessary to suppress diffraction into a $q\bar{q}g$ pair in which the gluon transverse momentum is not too small.

It would be nice if one could measure the jet momenta precisely enough so as to be able to identify the final nucleus as the target ground state. While it is very feasible to consider for eA colliders, this is impossible for high energy fixed target experiments, so another technique must be used here. The technique used in [14] is to isolate the dependence of the elastic diffractive peak on the momentum transfer to the target, t , as the distinctive property of the coherent processes. This was done by first introducing a cut on the momentum of the observed pions by requiring that they carry more than 90% of the incident momentum. This sample was then analyzed as a function of the total transverse momentum of the system. A strong coherent peak was observed with the slope consistent with the coherent contribution. The background was fitted as a sum of the coherent peak, inelastic diffraction with a nuclear break up and the term due to inelastic events where some hadrons were not detected.

The amplitude for the non-spin flip excitations of low-lying even-parity nuclear levels $\sim -t$, due to the orthogonality of the ground and excited state nuclear wave functions. Thus the cross section of these kinds of soft nuclear excitations integrated over t is suppressed by an additional factor of $1/R_A^4 \approx A^{-4/3}$ compared to the nuclear coherent process. For $\sqrt{-t} R_A \gg 1$ where q is the momentum transfer to the nucleus $q = \sqrt{-t}$ the background processes involving nuclear excitations vary as A , so an unwanted counting of such would actually weaken the signal we seek. For $qR_A \gg 1$ the diffractive peak cannot be used as signature of diffractive processes to distinguish them from non-diffractive processes whose cross section $\propto \sigma(\pi N) \propto A^{0.75}$. Thus substantial A -dependence, $\sigma \propto A^\alpha$ (with $\alpha \approx 1.5$), as predicted by QCD for large enough values of κ_t , should be distinguishable from the background processes.

The amplitude varies as $\mathcal{M}(A) \sim \alpha_s/\kappa_t^4$

$$\mathcal{M}(A) \sim \alpha_s x_N G_N(x_N, Q_{eff}^2)/\kappa_t^4, \quad (72)$$

where $Q_{eff}^2 \sim 2\kappa_t^2$. For the kinematics of the E791 experiment, where x_N increases $\propto \kappa_t^2$, the factor $\alpha_s x_N G_N(x_N, Q_{eff}^2)$ is a rather weak function of κ_t . For example, if we use the standard CTEQ5M parameterization we find $\sigma(A) \sim 1/\kappa_t^{8.5}$ for $1.5 \leq \kappa_t \leq 2.5$ GeV which is consistent with the data [14]. For the amplitude discussed here, $\sigma(A) \sim (z(1-z))^2$ which is in the excellent agreement with the data [14].

A. Extracting the coherent contribution

The experiment is discussed in Ref. [14]. The main advantage of this experiment is the excellent resolution of the transverse momentum. The reference also shows the identification of the dijet using the Jade algorithm, and it displays the identification of the diffractive peak by the q_t^2 dependence for very low q_t^2 . This dependence is consistent with that obtained from the previously measured radii $R(C) = 2.44$ fm, and $R_{Pt} = 5.27$ fm. The key feature is the identification of the coherent contribution from its rapid falloff with t .

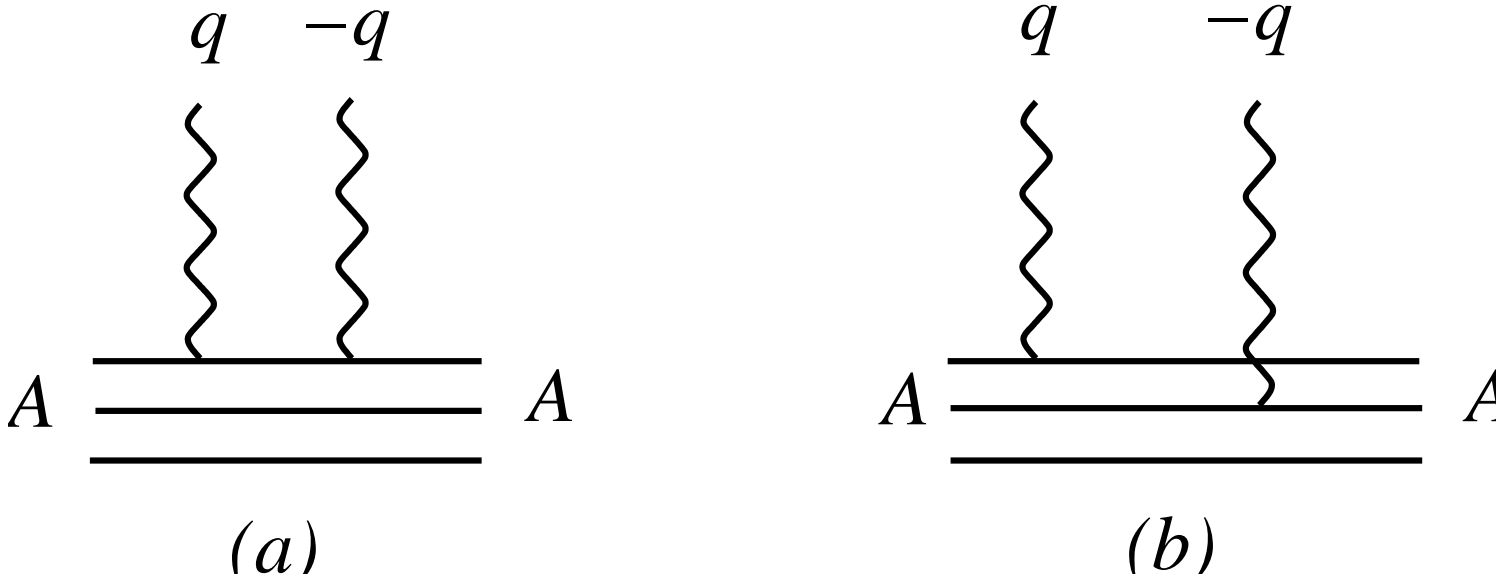


FIG. 13. Contributions to the total nuclear diffractive cross section. The wavy lines in this figure denote amplitude for the scattering of $q\bar{q}$ pair by a nucleon. (a) The terms with $i = j$. (b) $i \neq j$.

We discuss the extraction of this signal in some detail. We consider the contribution to the total cross section $\frac{d\sigma_A}{dt}$ that arises from the diffractive production of the dijet. The total cross section includes terms in which the final nucleus is not the ground state. The nuclear excitation energy is small compared to the energy of the beam, so that one may use closure to treat the sum over nuclear excited states. Then the cross section is evaluated as a ground state matrix element of an operator $\sum_{i,j} e^{i\mathbf{Q}\cdot(\mathbf{r}_i - \mathbf{r}_j)} = A + \sum_{i \neq j} e^{i\mathbf{Q}\cdot(\mathbf{r}_i - \mathbf{r}_j)}$; see Fig. 13. The result, obtained by using \mathbf{r}_i relative to the nuclear center of mass, and by neglecting correlations in the nuclear wave function is given by

$$\frac{d\sigma_A}{dt} = \left[A + A(A-1)F_A^2 \left(t \frac{A}{A-1} \right) \right] \frac{d\sigma_N}{dt}. \quad (73)$$

The factor $\frac{A}{A-1}$ in the argument of F_A is due to accounting for nuclear recoil in the mean field approximation, *cf.* [55]. This formula should be very accurate, for the small values of t relevant here. The contribution of the coherent processes to the total cross section is given by

$$\frac{d\sigma^{\text{coherent}}}{dt} = A^2 F_A^2(t) \frac{d\sigma_N}{dt}, \quad (74)$$

and the contribution of excited nuclear states is the difference: $\frac{d\sigma_A}{dt} - \frac{d\sigma^{\text{coherent}}}{dt}$, which vanishes at $t = 0$. The experiment proceeds by removing a term $\propto A$ from $\frac{d\sigma_A}{dt}$ which has no rapid variation with t . This defines a new cross section which is actually measured experimentally.

$$\frac{d\tilde{\sigma}_A}{dt} = A(A-1)F_A^2 \left(t \frac{A}{A-1} \right) \frac{d\sigma_N}{dt}. \quad (75)$$

The integral of this term over t can be extracted from the data:

$$\sigma_1 \equiv \int dt \frac{d\tilde{\sigma}_A}{dt} = \frac{3A(A-1)}{r_N^2 + R_A^2 \frac{A}{A-1}} \frac{d\sigma_N}{dt} \Big|_{t=0} \approx \frac{3(A-1)^2}{r_N^2 + R_A^2} \frac{d\sigma_N}{dt} \Big|_{t=0}. \quad (76)$$

Here the factor r_N^2 takes into account the slope of the elementary cross section, assuming that it is determined solely by the nucleon vertex. Note that the result (76) differs by a factor of $\frac{(A-1)^2}{A^2}$ from the A -dependence predicted previously

for coherent processes, recall Eq. (66). Using $A=12, 195$, the nuclear radii mentioned above, $r_N = 0.83 fm$ and fitting the ratio of cross sections obtained from Eq.(76) with the parametrization $\sigma \propto A^\alpha$, gives then

$$\alpha = 1.54, \tag{77}$$

instead of $\alpha = 1.45$.

The result [14] of the experiment is

$$\alpha \approx 1.55 \pm 0.05, \tag{78}$$

which is remarkably close to the theoretical value shown in Eq. (77). The sizes of our multiple scattering and nuclear shadowing corrections, which work in the opposite directions, and which were discussed in the previous Section, are of the order of the experimental error bar.

VII. ELECTROMAGNETIC BACKGROUND

Because very low values of q_t^2 are involved, one could ask if the process occurs by a one-photon exchange (a type of Primakoff effect) instead of a two-gluon exchange. If the momentum transfer is very low, the process is peripheral and there would be no initial or final state interactions. Thus, it is necessary to estimate the relative importance of the two effects.

This amplitude is caused by the exchange of a virtual photon of four-momentum q ($q^2 = t$) with the target. The nuclear Primakoff amplitude is then given by

$$\mathcal{M}_P(A) = e^2 \frac{\langle \pi | J_\mu^{\text{em}} | q\bar{q} \rangle}{-t} (P_A^i + P_A^f)^\mu \frac{Z}{A} F_A(t) \approx 2e^2 \langle \pi | J^{\text{em}} \cdot \frac{P_A}{A} | q\bar{q} \rangle \frac{Z F_A(t)}{-t}, \tag{79}$$

where we will use the decomposition $-t = q^2 = q_t^2 - t_{\text{min}}$. A photon can be attached to any charged particle, so a direct calculation would involve a complicated sum of diagrams. We may simplify the calculation by using the fact that the electromagnetic current is conserved. This application is simplified by the use of Sudakov variables, which is a necessary first step. Accordingly, we write

$$q = \alpha \frac{P_A}{A} + \beta p_\pi + q_t. \tag{80}$$

Conservation of four-momentum gives

$$\beta = \frac{q^2}{2(p_\pi \cdot P_A)}, \quad \alpha = \frac{-m_f^2}{s}. \tag{81}$$

Then conservation of current can be written as

$$\langle \pi | J^{\text{em}} \cdot q | q\bar{q} \rangle \approx \alpha \langle \pi | J^{\text{em}} \cdot \frac{P_A}{A} | q\bar{q} \rangle + \beta \langle \pi | J^{\text{em}} \cdot p_\pi | q\bar{q} \rangle - \langle \pi | J^{\text{em}} \cdot q_t | q\bar{q} \rangle = 0. \tag{82}$$

The use of Eq. (81) and keeping only the leading term in μ^2/s , where μ is the typical mass involved in the considered process, allows us to neglect the β term of Eq. (82) so that

$$\alpha \langle \pi | J^{\text{em}} \cdot \frac{P_A}{A} | q\bar{q} \rangle = \langle \pi | J^{\text{em}} \cdot q_t | q\bar{q} \rangle \tag{83}$$

By definition, the transverse momentum of a pion is zero, so the dominant (in terms of powers of κ_t) contribution in Eq. (83) is given by photon attachments to quark lines, and the matrix element is given by ³

$$\langle \pi | J^{\text{em}} \cdot q_t | q\bar{q} \rangle = \chi_\pi(z, \kappa_t) q_t \cdot \kappa_t (2/3z - 1/3(1-z)). \tag{84}$$

³The above (84) differs from that of the first version of our paper which appeared in hep-ph. We are indebted to D.Ivanov and L.Szczymanowsky - who drew our attention to the misprint in this version of the paper.

The generalization of this result to account for all Feynman diagrams having the same powers of s and κ_t^2 is almost trivial. The relative contribution of other diagrams is $\propto k'_t/\kappa_t$ where k'_t is the transverse momentum of quarks in the intermediate state. But within the $\alpha_s \ln \kappa_t^2/\Lambda_{QCD}^2$ approximation $k_t^2 \ll \kappa_t^2$ so this contribution does not lead to a $\ln \kappa_t^2/\Lambda_{QCD}^2$ term. Thus the above formula is valid within the $\alpha_s \ln \kappa_t^2/\Lambda_{QCD}^2$ approximation when $\alpha_s \ll 1$.

The net result, obtained by using Eq. (83) in Eq. (79), is

$$\mathcal{M}_P(A) = \frac{-e^2 \chi_\pi(z, \kappa_t) Z}{q_t^2 - t_{\min}} F_A(t) \frac{s}{k_t^2} 2q_t \cdot \kappa_t (2/3 - z) \quad (85)$$

which should be compared with the amplitude of Eq. (64) (including the effect of the nuclear form factor, which enters at non-zero values of t , but ignoring the logarithmic correction) written as

$$\mathcal{M}(A) = -i \chi_\pi(z, \kappa_t) A \frac{s \sigma_0 \nabla_{k_t}^2}{\langle b^2 \rangle} F_A(t) \approx 4i \chi_\pi(z, \kappa_t) / k_t^2 A \frac{s \sigma_0}{\langle b^2 \rangle} F_A(t) \quad (86)$$

The Primakov term has been evaluated also in the paper of D.Ivanov and L.Sczymanowsky [62]. As the consequence of different approximations result obtained in [62] differs from ours. We use conservation of the e.m. current to deduce the Weizecker-Williams approximation and to account for the cancellation between diagrams corresponding to attachments of photon to the different charged constituents of a pion. After accounting for the cancellation we restrict ourselves by the contribution of diagrams enhanced by the large factor κ_t from the vertex of quark(antiquark)-photon interaction. Dominance of photon interaction with external quark lines in the pion fragmentation into 2 jets is another form of the QCD factorization theorem which properly accounts for the conservation of the e.m. current and the gauge invariance of QCD. On the contrary [62] interacting particles are put on mass shell before the separation of scales and the cancellations between different photon attachments has been taken into account. These approximations have problems with the conservation of the e.m.current and the renormalization group in QCD.

The ratio of electromagnetic and strong amplitudes is given by

$$\frac{\mathcal{M}_P(A)}{\mathcal{M}(A)} = -i e^2 \frac{Z}{A} \frac{2/3 - z}{\sigma_0 / \langle b^2 \rangle} \frac{q \cdot \kappa_t}{2(q_t^2 - t_{\min})} \quad (87)$$

Using $q_t^2 \approx 0.02 \text{ GeV}^2$ (the smallest value measured in [14] $Z/A=1/2$, $e^2 = 4\pi/137$, $\kappa_t = 2 \text{ GeV}$, $\sigma_0 / \langle b^2 \rangle \approx 2.5$ (this is 1/4 of the value of Ref. [5]), and taking q_t parallel to κ_t we find that

$$\frac{\mathcal{M}_P(N)}{\mathcal{M}(N)} \approx -1/8(2/3 - z) i \approx -0.02 i, \quad (88)$$

with $z = 1/2$.

Thus the Primakoff term is very small and, because of its real nature, interference with the larger strong amplitude (which is almost purely imaginary) is additionally suppressed. We may safely ignore this effect for the energy range of Ref. [14], or any contemplated fixed target experiment. At collider energies, it will be possible to measure jets of much larger values of transverse momentum, so any complete theoretical analysis should account for this electromagnetic interaction.

For a heavy nuclei target another electromagnetic process $\propto Z^2 \alpha_{em}^2$ in the amplitude gives a contribution. This is a dijet production due to the two-photon exchange, a version of Fig. 8 in which the exchanged gluons are replaced by exchanged photons. For small transverse momenta of quarks $l_t^2 \ll \kappa_t^2$ in the pion wave function, this contribution is suppressed as the power of s in the amplitude. This is because, in the calculation of the imaginary part of the diagram, x_2 for the exchanged photon is given by

$$x_2 \nu = -\frac{k_t^2}{z}, \quad (89)$$

except for a very narrow region of z near $z = 0, 1$, which is suppressed by the decrease of the pion wave function. Thus $x_2 < 0$ and according to our previous arguments, this contribution should be very small. For large l_t this contribution may also be expressed in terms of the same pion wave function as in the case of the two-gluon exchange. It is easy to estimate this EM amplitude obtained from the two-photon exchange:

$$\mathcal{M}(\gamma\gamma) = \alpha_{em}^2 (s/k_t^2) \chi(z, k_t) \pi Z^2 \int \frac{d^2 l_t}{l_t^2} F_A(l_t) F_A(q_t - l_t) (8e_1 e_2) (1 - 2z). \quad (90)$$

Here $e_1(e_2)$ is electric charge of quark (anti-quark) in the units of the electric charge of electron. The lower limit of integration over l_t^2 is $(\kappa_t^2/2z(1-z))^2$. Thus the contribution of this term to the cross section should have the same z and κ_t^2 dependence as the two-gluon exchange term, but with a much faster Z dependence ($\propto Z^4$). This term is negligible also.

VIII. DISCUSSION AND SUMMARY

The use of the experimentally measured [14] value of $\alpha = 1.55$ (recall Eq. (70)) leads to

$$\frac{\sigma(Pt)}{\sigma(C)} = 75. \quad (91)$$

The typical usual nuclear dependence of the soft diffractive processes observed in the high energy processes is $\approx A^{2/3}$ or $\alpha = 2/3$. The use of a Glauber approximation with a typical hadronic cross section for the final system tends to predict the A dependence as $\approx A^{1/3}$. An account of color fluctuations [56] predicts $\approx A^{2/3}$, in agreement with the FNAL data [57] which would give

$$\frac{\sigma_{\text{USUAL}}(Pt)}{\sigma_{\text{USUAL}}(C)} = 7. \quad (92)$$

Thus color transparency causes a factor of 10 enhancement! This seems to be the huge effect of color transparency that many of us have been hoping to find. It is also true that, as noted in the Introduction, that the κ_t and z dependence of the cross section [14] is in accord with our prediction.

All of this looks very good, but it is necessary to provide some words of caution. Our analysis was related to a nuclear coherent process involving a $q\bar{q}$ final state. If the experimental signal is significantly contaminated by incoherent nuclear effects or by $q\bar{q}g$ final states, our analysis might not be applicable. However, the experimental [14] extraction of the coherent peak using the q_t^2 dependence of the amplitude, and the measurement of the two-jet (as opposed to three-jet) cross section seem very secure to us, except for the small correction discussed in Sect. V. Another worry is that the color transparency effect seen in Ref. [14] seems to start for values of κ_t near 1 GeV. These are lower than suggested in Ref. [5]. These earlier predictions used modeling of non-perturbative effects, and such modeling may be necessary to guess the lowest values of κ_t for which color transparency would occur. The reasoning of the present paper uses perturbative QCD, which becomes more reliable as κ_t increases. This is because the competing amplitudes $T_{2,3,4}$ are decreased relative to T_1 by a factor of $\frac{A^2}{\kappa_t^2}$ ($\approx .04$ for $\kappa_t = 1$ GeV) or $\alpha_s(\kappa_t^2)$. A coherent sum of the sub-dominant amplitudes could provide a significant correction to our dominant pure amplitude. However, the observed falloff of the cross section with κ_t , combined with the z and A dependence, does provide very strong evidence for color transparency.

It is worth noting similarities and differences between the process we discuss in this paper and another factorizable process, that of hard exclusive electroproduction of mesons [36,58]. Both processes allow a simple geometric interpretation in the transverse coordinate representation: a convolution of the initial wave short-distance wave function, $\psi_{in}(z, b)$, the dipole-target cross section, $\sigma(b, x)$, and the final wave function $\psi_{fin}(b, z)$. However, in the case of the vector meson production, the Q^2 dependence of the longitudinal photon wave function at small b causes the final vector meson wave function to be evaluated at $b \approx 2/Q$. In the case of the pion dijet diffraction the pion wave function enters at small values of $b \sim \frac{1}{\kappa_t}$.

If color transparency has been correctly observed in the $\pi + A \rightarrow q\bar{q} + A$ (ground state), there would be many implications. The spectacular enhancement of the cross section would be a novel effect. The point-like configurations would be proved to exist. This would be one more verification of the concept and implications of the idea of color. Furthermore, the definitive proof of the existence of color transparency means that we now have available a new effective tool to investigate microscopic hadron, nuclear structure at hundreds of GeV energy range. At lower energies of a ten's of GeV color transparency is masked to some extent by the diffusion of a spatially small quark-gluon wave package to the normal hadronic size [12]. Still it is possible that previous experiments [59] showing hints [60] of color transparency (for a review see Ref [12]) probably do show color transparency. Efforts [61] to observe color transparency at Jefferson Laboratory, and at HERMES(DESY) should be increased. The electron-ion collider would provide numerous possibilities for studying color transparency both in di-, tri-jet coherent production as well as in exclusive processes.

The observation of CT confirms the idea that the life span of the perturbative phase can be increased by the large Lorentz factor associated with high energy beams. A challenging problem would be to explore this idea to observe the perturbative phase in a "macroscopic" volume. One manifestation of this would be the production of huge blob-like configurations of Huskyons [63]. These different configurations have wildly different interactions with a nucleus [64], so that the nucleon in the nucleus can be very different from a free nucleon. More generally, the idea that a nucleon is a composite object is emphasized by these findings. Some configurations of the nucleon interact very strongly with the surrounding nucleons; some interact very weakly. This means that the nucleon in the nucleus can be very different from a free nucleon. This leads to an entirely new view of the nucleus, one in which the nucleus is made out of oscillating, pulsating, vibrating, color singlet, composite objects.

The technical purpose of this paper has been to show how to apply leading-order perturbative QCD to computing the scattering amplitude for the coherent processes: $\pi N \rightarrow JJ N$ and $\pi A \rightarrow JJ A$. The high momentum component of the pion wave function, computable in perturbation theory, is an essential element of the amplitude. The dominance of the amplitude of the T_1 term of Eq. (64) is obtained by showing that the corrections to it, which at first glance seem to be of the same order in the coupling constant, are vanishingly small. This vanishing, obtained using arguments based on analyticity, causality, and current conservation, is equivalent to the verification of a specific space-time description of the event: the pion produces its point-like component at distances well before the target. Furthermore, for the conditions of the experiment [14] studied here, the competing electromagnetic production process is shown to yield a negligible effect. It seems that perturbative QCD can be applied to the coherent nuclear production of high-relative momentum dijets by high energy pions.

It therefore seems interesting to consider similar reactions involving other projectiles such as photons, kaons, and protons. The observations of the coherent photoproduction of the J/ψ from nuclear targets has long been known [65] to have an A dependence which is very similar to that observed here, but the authors of [65] did not interpret it as color transparency phenomenon. Later on H1 and ZEUS detectors at HERA investigated exclusive photoproduction of the J/ψ meson from a proton target. The striking qualitative predictions for this process based on the QCD factorization theorem, such as energy and t dependence, are in accordance with the data; for a recent review see [1,66]. Thus now there exist serious reasons to believe that color transparency phenomenon has been observed in the combination of coherent photoproduction of J/ψ from nuclei(FNAL) and from the nucleon (HERA). Our present theory can be used for kaon projectiles with little modification. Because the kaon has a smaller size than the pion, we expect that the amplitude for a kaon-induced process should be somewhat larger than that of the pion induced process discussed here. The same analysis should be applicable to the photoproduction of high κ_t $q\bar{q}$ pair of light quarks. It is important here that the contribution of bare photon coupling to the $q\bar{q}$ is proportional to quark's bare mass and is negligible for forward scattering [31,32]. The contribution of a target gluon with $k_{it}^2 \approx \kappa_t^2$ discussed in [32] is suppressed by Sudakov and w_2 form factors discussed above. However, the PQCD physics of light quarks will be masked to some extent by another striking prediction of QCD, which is the enhancement of the diffractive production of charmed dijets because of a large bare mass of charmed quarks.

The study of high energy coherent production of jet systems from nuclear targets seems to be a very productive way to investigate both perturbative QCD and microscopic nuclear structure by exploring the diverse effects of color transparency. Such studies in the region of hundreds of GeV seem ideally suited for the non-destructive investigation of a microscopic hadron, and nuclear structure. It may be possible to remove a piece of hadron ($q\bar{q}$ pair..) or to implant (strangeness in the center of a nucleus...) without destruction of a target. Such investigations resemble modern methods of surgery which avoid cutting muscles. So it seems appropriate to name this new field of investigations as micro-surgery of a hadron, or of a nucleus.

ACKNOWLEDGMENTS

We would like to thank S.Brodsky, J.Collins, Yu.Dokshitzer and A.Mueller for the useful discussions. This work has been supported in part by the USDOE and GIF.

-
- [1] H. Abramowicz and A. Caldwell, Rev. Mod. Phys. **71**, 1275 (1999).
 - [2] S. F. King, A. Donnachie and J. Randa, Nucl. Phys. **B167**, 98 (1980);
J. Randa, Phys. Rev. **D22**, 1583 (1980).
 - [3] G.F. Bertsch, S.J. Brodsky, A.S. Goldhaber, and J.F. Gunion, Phys. Rev. Lett. **47**, 297 (1981).
 - [4] Reference [3] stated that “*The exponential suppression we obtained in eq.(13) is of course a many-body effect, with validity limited to nuclear targets and low to moderate k_\perp . In the regime where the jet structure is visible, the pion induced jets will have the angular dependence in the jet c.m. frame of $d\sigma/dM^2 d\cos\theta \approx \sin^2\theta$, reflecting the x dependence of*” the equation for the pion wave function. Thus Ref. [3] implied that k_t dependence will obey a power law form: k_\perp^{-6} of [2], which is different from the form k_\perp^{-8} deduced in this paper. The conclusion Ref. [3] explicitly formulated is that “*the nuclear filter does not generally produce states with large enough k_\perp that a jet structure is expected to appear.*”
 - [5] L. Frankfurt, G.A. Miller, and M.Strikman, Phys. Lett. **B304** 1, (1993).
 - [6] V. N. Gribov, “Lectures On The Theory Of Complex Momenta,” KHFTI-PREPRINT-70-47; V. N. Gribov, L. N. Lipatov, and G. V. Frolov, Sov. J. Nucl. Phys. **12**, 543 (1971).

- [7] Feynman, R.P. PHOTON - HADRON INTERACTIONS. By R.P. Feynman. Benjamin, 1972.
- [8] V. N. Gribov and L. N. Lipatov, *Yad. Fiz.* **15**, 781 (1972) [*Sov. J. Nucl. Phys.* **15**, 438 (1972)].
- [9] Y. L. Dokshitzer, *Sov. Phys. JETP* **46**, 641 (1977).
- [10] E. A. Kuraev, L. N. Lipatov, and V. S. Fadin, *Sov. Phys. JETP* **45**, 199 (1977) [*Zh. Eksp. Teor. Fiz.* **72**, 377 (1977)].
I. I. Balitsky and L. N. Lipatov, *Sov. J. Nucl. Phys.* **28**, 822 (1978) [*Yad. Fiz.* **28**, 1597 (1978)].
- [11] L. Frankfurt, A. Freund, V. Guzey, and M. Strikman, *Phys. Lett. B* **418**, 345 (1998) [Erratum-ibid. *B* **429**, 414 (1998)] [[hep-ph/9703449](#)].
- [12] See the review: L.L. Frankfurt, G.A. Miller and M. Strikman, *Ann. Rev. Nucl. Part. Sci.* **44**, 501 (1994) [[hep-ph/9407274](#)].
- [13] F.E. Low, *Phys. Rev.* **D12**, 163 (1975).
- [14] E. M. Aitala *et al.* [Fermilab E791 Collaboration], *Phys. Rev. Lett.* **86**, 4773 (2001); E. M. Aitala *et al.* [Fermilab E791 Collaboration], *Phys. Rev. Lett.* **86**, 4768 (2001).
- [15] Is it interesting to note that soft diffraction cross sections vary as $A^{0.8}$, which is a higher power than the $\sim A^{1/3}$ expected from edge effects which one would expect for the case of scattering from a black body. A faster A dependence arises from the significant fluctuations in the strength of pion-nucleon interaction (for a review and references see [12]).
- [16] J. C. Collins, L. Frankfurt and M. Strikman, *Phys. Rev.* **D56**, 2982 (1997) [[hep-ph/9611433](#)].
- [17] L. Frankfurt, G. A. Miller and M. Strikman, *Found. Phys.* **30**, 533 (2000)
- [18] B. Blattel, G. Baym, L. L. Frankfurt and M. Strikman, *Phys. Rev. Lett.* **70**, 896 (1993).
- [19] L. Frankfurt, V. Guzey and M. Strikman, *J. Phys. G* **27**, R23 (2001) [[arXiv:hep-ph/0010248](#)].
- [20] L. L. Frankfurt, M. I. Strikman and S. Liuti, *Phys. Rev. Lett.* **65**, 1725 (1990).
- [21] T. Gousset and H. J. Pirner, *Phys. Lett. B* **375**, 349 (1996) [[hep-ph/9601242](#)].
- [22] K. J. Eskola, V. J. Kolhinen and C. A. Salgado, *Eur. Phys. J.* **C9**, 61 (1999) [[hep-ph/9807297](#)].
- [23] L. Frankfurt and M. Strikman, *Eur. Phys. J.* **A5**, 293 (1999).
- [24] M. Arneodo *et al.* [New Muon Collaboration], *Nucl. Phys. B* **481**, 23 (1996).
- [25] L. Frankfurt, W. Koepf, M. Strikman, *Phys. Rev.* **D54**, 3194 (1996); M. McDermott, L. Frankfurt, V. Guzey and M. Strikman, [[hep-ph/9912547](#)].
- [26] M. Vanderhaeghen, P. A. Guichon and M. Guidal, *Phys. Rev. Lett.* **80**, 5064 (1998).
- [27] V. N. Gribov and A. A. Migdal, *Sov. J. Nucl. Phys.* **8**, 583 (1969);
J. B. Bronzan, G. L. Kane and U. P. Sukhatme, *Phys. Lett.* **B49**, 272 (1974).
- [28] G. 't Hooft, *Nucl. Phys.* **B33**, 173 (1971); G. 't Hooft, *Nucl. Phys.* **B35**, 167 (1971); G. 't Hooft and M. Veltman, *Nucl. Phys.* **B44**, 189 (1972).
- [29] L. Frankfurt and M. Strikman, *Prog. Part. Nucl. Phys.* **27**, 135 (1991).
- [30] Y. L. Dokshitzer, V. A. Khoze, and S. I. Troyan, in *Proceedings of the 6th Int. Conference on Physics in Collisions 1986*, ed M. Derrick (World Scientific, Singapore, 1987), p. 365;
H. Bengtsson and T. Sjostrand, *Comput. Phys. Commun.* **46**, 43 (1987);
Y. L. Dokshitzer, V. A. Khoze, S. I. Troian and A. H. Mueller, *Rev. Mod. Phys.* **60**, 373 (1988).
- [31] S. J. Brodsky and J. Gillespie, *Phys. Rev.* **173**, 1011 (1968).
- [32] M. Diehl, *Z. Phys. C* **66**, 181 (1995) [[hep-ph/9407399](#)].
- [33] V.B.Berestetskii, E.M. Lifshitz, L.P. Pitaevskii *Quantum Electrodynamics*. 2nd ed. Pergamon Press, 1982. 652p. (Course of Theoretical Physics, v. 4)
- [34] Hung Cheng and Tai Tsun Wu, *Expanding Protons: scattering at high energies*, MIT Press, 1987. 285p.
- [35] F.E. Low, *Phys. Rev.* **110**, 974 (1958).
- [36] S. J. Brodsky, L. Frankfurt, J. F. Gunion, A. H. Mueller and M. Strikman, *Phys. Rev.* **D50**, 3134 (1994).
- [37] Each Feynman graph shown in our figures consists of a sum of different graphs corresponding to different time orderings. When we define a given intermediate state, we are concerned with a given time ordering, and will find it necessary to consider other time orderings of the same Feynman graph.
- [38] V. M. Braun, D. Y. Ivanov, A. Schafer and L. Szymanowski, *Phys. Lett. B* **509**, 43 (2001).
- [39] G. Ingelman and P. E. Schlein, *Phys. Lett. B* **152**, 256 (1985).
- [40] C. Adloff *et al.* [H1 Collaboration], *Eur. Phys. J. C* **20**, 29 (2001) [[arXiv:hep-ex/0012051](#)].
- [41] J. C. Collins, L. Frankfurt and M. Strikman, *Phys. Lett. B* **307**, 161 (1993) [[arXiv:hep-ph/9212212](#)].
- [42] B.K. Jennings and G.A. Miller *Phys.Rev.* **C50**, 3018 (1994).
- [43] J. M. Cornwall and G. Tiktopoulos, *Phys. Rev. D* **15**, 2937 (1977).
R. Coquereaux and E. de Rafael, *Phys. Lett. B* **69**, 181 (1977).
- [44] Y. L. Dokshitzer, D. Diakonov and S. I. Troian, *Phys. Rept.* **58**, 269 (1980).
- [45] N. N. Nikolaev, W. Schafer and G. Schwiete, [[hep-ph/0009038](#)] *Phys. Rev. D* **63**, 014020 (2001).
- [46] S.J. Brodsky G.P. Lepage, *Phys. Rev.* **D22**, 2157 (1982)
- [47] A. V. Efremov and A. V. Radyushkin, *Phys. Lett. B* **94**, 245 (1980). G. P. Lepage and S. J. Brodsky, *Phys. Lett. B* **87**, 359 (1979).
- [48] A.V. Radyushkin, [[hep-ph/9707335](#)]; A. Szczepaniak, A. Radyushkin and C. Ji, *Phys. Rev.* **D57**, 2813 (1998) [[hep-ph/9708237](#)]; I.V. Musatov and A.V. Radyushkin, *Phys. Rev.* **D56**, 2713 (1997) [[hep-ph/9702443](#)].
- [49] P. Kroll and M. Raulfs, *Phys. Lett.* **B387**, 848 (1996) [[hep-ph/9605264](#)].

- [50] L. Frankfurt, A. Radyushkin, and M. Strikman, Phys. Rev. **D55**, 98 (1997)
- [51] L. Mankiewicz, G. Piller and T. Weigl, Eur. Phys. J. C **5**, 119 (1998) [arXiv:hep-ph/9711227].
- [52] A. Freund, V. Guzey, hep-ph - 9801388; Phys. Lett. B **462**, 178 (1999) [arXiv:hep-ph/9806267].
- [53] H. Abramowicz, L. Frankfurt and M. Strikman, SLAC Summer Inst.1994:0539-574, Surveys High Energy. Phys. **11**, 51 (1997) [hep-ph/9503437].
- [54] A. V. Radyushkin, Phys. Rev. **D59**, 014030 (1999)
- [55] R. H. Bassel, and C. Wilkin, Phys.Rev. **174** 1179 (1968).
- [56] L. Frankfurt, G. A. Miller and M. Strikman, Phys. Rev. Lett. **71**, 2859 (1993) [hep-ph/9309285].
- [57] M. Zielinski *et al.*, Z. Phys. **C16**, 197 (1983).
- [58] J. C. Collins, L. Frankfurt and M. Strikman, Phys. Rev. D **56**, 2982 (1997) [hep-ph/9611433].
- [59] A.S. Carroll *et al.*, Phys. Rev. Lett. **61**, 1698 (1988);
- [60] B.K. Jennings and G.A. Miller, Phys. Rev. Lett. **69**, 3619 (1992);
 B.K. Jennings and G.A. Miller, Phys. Lett. **B236**, 209 (1990);
 B.K. Jennings and G.A. Miller, Phys. Rev. **D44**, 692 (1991);
 B.K. Jennings and G.A. Miller, Phys. Lett. **B318**, 7 (1993).
- [61] K. Egiyan, L. Frankfurt, W.R. Greenberg, G.A. Miller, M. Sargsian and M. Strikman, Nucl. Phys. **A580**, 365 (1994);
 L.L. Frankfurt, W.R. Greenberg, G.A. Miller, M.M. Sargsian and M.I. Strikman, Z. Phys. **A352**, 97 (1995); L. Frankfurt,
 W.R. Greenberg, G.A. Miller, M.M. Sargsian and M.I. Strikman, Phys. Lett. **B369**, 201 (1996) .
- [62] D. Y. Ivanov and L. Szymanowski, Phys. Rev. D **64**, 097506 (2001) [arXiv:hep-ph/0103184].
- [63] A. Bulgac and L. Frankfurt, Phys. Rev. **D48** (1993) 1894.
- [64] L.L. Frankfurt and M.I. Strikman, Nucl. Phys. **B250**, 143 (1985). M.R. Frank, B.K. Jennings and G.A. Miller, Phys. Rev. **C54**, 920 (1996).
- [65] M. D. Sokoloff *et al.* [Fermilab Tagged Photon Spectrometer Collaboration], Phys. Rev. Lett. **57**, 3003 (1986).
- [66] M. Wusthoff and A. D. Martin, J. Phys. **G25**, R309 (1999) [hep-ph/9909362].